Decomposing sources of uncertainty in climate change projections of boreal forest primary production

Tuomo Kalliokoski[1,2*] Annikki Mäkelä[2], Stefan Fronzek[3], Francesco Minunno[2], Mikko Peltoniemi[4]

1 University of Helsinki, Department of Physics, P.O. Box 64, FI-00014 University of Helsinki

2 University of Helsinki, Department of Forest Sciences, P.O. Box 27, 00014 University of Helsinki

3 Finnish Environment Institute, P.O. Box 140 Helsinki

4 Natural Resources Institute Finland, Latokartanonkaari 9, FI-00790 Helsinki

*Corresponding author: tuomo.kalliokoski@helsinki.fi, +358 50 4487536

Highlights

- We predict GPP and water balance of Finnish forests by simple ecosystem model PRELES
- We show how different sources of uncertainty propagates to ecological impacts.
- Global Circulation Model (GCM) variability was the major source of uncertainty until 2060.
- We need to improve our mechanistic understanding of long-term CO_2 fertilization effect on GPP.
- A thorough assessment of uncertainties in the projections of the impacts is important for drawing robust conclusions.

Abstract

We are bound to large uncertainties when considering impacts of climate change on forest productivity. Studies formally acknowledging and determining the relative importance of different sources of this uncertainty are still scarce, although the choice of the climate scenario, and e.g. the assumption of the CO_2 effects on tree water use can easily result in contradicting conclusions of future forest productivity. In a large scale, forest productivity is primarily driven by two large fluxes, gross primary production (GPP), which is the source for all carbon in forest ecosystems, and heterotrophic respiration. Here we show how uncertainty of GPP projections of Finnish boreal forests divides between input, mechanistic and parametric uncertainty. We used the simple semi-empirical stand GPP and water balance model PRELES with an ensemble of downscaled global circulation model (GCM) projections for the 21st century under different emissions and forcing scenarios (both RCP and SRES). We also evaluated the sensitivity of assumptions of the relationships between atmospheric CO_2 concentration (C_a), photosynthesis and water use of trees. Even mean changes in climate projections of different meteorological variables for Finland were so high that it is likely that the primary productivity of forests will increase by the end of the century. The scale of productivity change largely depends on the long-term C_a fertilization effect on GPP and transpiration. However, GCM variability was the major source of uncertainty until 2060, after which emission scenario/pathway became the dominant factor. Large uncertainties with a wide range of projections can make it more difficult to draw ecologically meaningful conclusions especially on the local to regional scales, yet a thorough assessment of uncertainties is important for drawing robust conclusions.

KEY WORDS: Photosynthetic efficiency, Ecosystem response, Environmental change, Ecophysiology

1. INTRODUCTION

Understanding the development of forest productivity in a changing environment is pivotal for making decisions about forest use in the future. Such understanding is also needed for improving the climate projections themselves, as a large proportion of uncertainty of global warming projections arises from uncertainties in modelling terrestrial phenomena and their biophysical interactions with climate (Bonan 2008). Boreal forests play a large role in determining the global mean temperature (Snyder et al. 2004, Snyder and Liess 2014), and are generally assumed to provide climate mitigation potential due to projected increased growth and carbon sequestration under climate change (IPCC 2013), although the biophysical effects like albedo or biogenic volatile organic compounds (BVOCs) may change the net impact (Bright 2014, Unger 2014). Opposing trends may also emerge as a result of increased utilization of forests for the production of bioenergy and new bio-based products (Ollikainen 2014). For example in Finland, recent impact studies suggest an increase of 5-27% in productivity of Norway spruce until end of this century (Ge et al. 2013 using SRES A2 scenarios, Reyer et al. 2014 using SRES A1B). However, all impact studies include a lot of uncertainty related to model structure, parameter values, and climate input data, which has not been systematically analysed in boreal forest studies. The lack of including these in the assessment of uncertainty may lead to suboptimal decision-making from the climate change mitigation perspective.

In a large scale comparison, forest productivity is primarily driven by two large fluxes, gross primary production (GPP), which is the source carbon for all carbon in forest ecosystems (Ma et al. 2015), and heterotrophic respiration. Correlations can therefore be found along environmental gradients between GPP and Net Primary Production (NPP; Waring et al. 1998, Mäkelä and Valentine 2001, Dewar et al. 1998), litter fall (Reich et al. 2014, Mäkelä et al. 2016) and carbon accumulation in the soil (Liski et al. 2006). Recent decades have witnessed a profound development of models of canopy GPP, thanks to improved measurements and data from eddy flux networks where carbon and water fluxes are measured globally over different land cover types (e.g.FLUXNET, https://fluxnet.fluxdata.org). This has

considerably improved the reliability of GPP predictions under current climate as a function of weather and canopy type (e.g. Novick et al. 2015, Wagle et al. 2016), sometimes also with generic models that do not require site-specific parameterisation (Minunno et al. 2016). Model-data assimilation techniques such as Bayesian model calibration also provide an improved understanding of the uncertainties of model parameters and how they propagate to model predictions (van Oijen et al. 2013, Minunno et al. 2016). The significance of GPP for ecosystem functioning, combined with a sound understanding of the process under the current climate, makes GPP simulatons an appropriate example case for exploring the types of uncertainty we are bound to face in future impact projections in a changing climate.

Uncertainties in model predictions generally originate in input uncertainty and model uncertainty (cf. Uusitalo et al. 2015). In climate change projections, input uncertainty includes uncertainties about climate scenario and climate development under a given scenario, demonstrated in the differences between climate models. In addition, there is uncertainty caused by natural variability of weather. Model uncertainty consists of parametric and structural uncertainty.

An important structural uncertainty for GPP prediction arises from the fact that the interactions of elevated atmospheric CO_2 concentrations (C_a) with changing climate are still poorly understood due to the limited possibilities of theory and model testing in experimental and natural conditions. In modelling studies, even more than half of the projected forest productivity has been attributed to increasing C_a (Bergh et al. 2005, Reyer et al. 2014) while without C_a fertilization, simulated forest productivity has even been predicted to decrease under climate change (Ollinger et al. 2007, Medlyn et al. 2011). While it is generally accepted that elevated C_a increases the water use efficiency of plants (WUE), the extent and mechanisms of this effect are not clear. Analyses of eddy-covariance measurements of the past 15 years have suggested even larger improvements of WUE than predicted by prevailing theories (Keenan et al. 2013). While studies where C_a concentration has been increased in the field (Free-Air Carbon dioxide Enrichment, FACE) have shown that trees increase their photosynthetic rates and still reduce stomatal conductance (Ainsworth and Rogers 2007), the long-term ecosystem level responses depend on ecosystem type. Direct responses of trees to elevated C_a may become diluted in time, as physiological processes and tree structure acclimate to new conditions (Norby and Zak 2011). For example, some

studies have predicted spruce decline in southern Finland (Kellomäki et al. 2008, Ge et al. 2013), but the result strongly depends on the assumptions of C_a effects on transpiration.

The impact uncertainty arising from uncertainties in global circulation model (GCM) outputs has largely been ignored in (forest productivity in the boreal zone, although it has been investigated in the context of e.g. disturbances (Lehtonen et al. 2016). It is well known that projections of climate models can differ more between each other than projections of one specific climate model between emission scenarios (e.g. van Vuuren et al. 2011, Ahlström et al. 2012, Nishina et al. 2015). In the case of Finland, only few GCMs project mean annual temperature changes below 2 ºC between the periods 1971-2000 and 2070-2099, even when assuming a low emission scenario (SRESB1) or a low emission Representative Concentration Pathway (RCP2.6) (Fig.1). The respective changes in the high-end scenarios reach up to 10 ºC (under RCP8.5 forcing, see Jylhä et al. 2009, Rötter et al. 2013, Ruosteenoja et al. 2016). The change in winter temperatures in January may be twice as large as the change in summer temperatures in July. Uncertainties in precipitation changes are much larger, but increases are expected especially in winter (Rötter et al. 2013, Jylhä et al. 2009). The frequent approach of using the ensemble mean of climate model variables as input to ecosystem models (e.g. Peltola et al. 2010, Veijalainen et al. 2010, Sievänen et al. 2014) is questionable since it may violate the coherence between different climate variables.

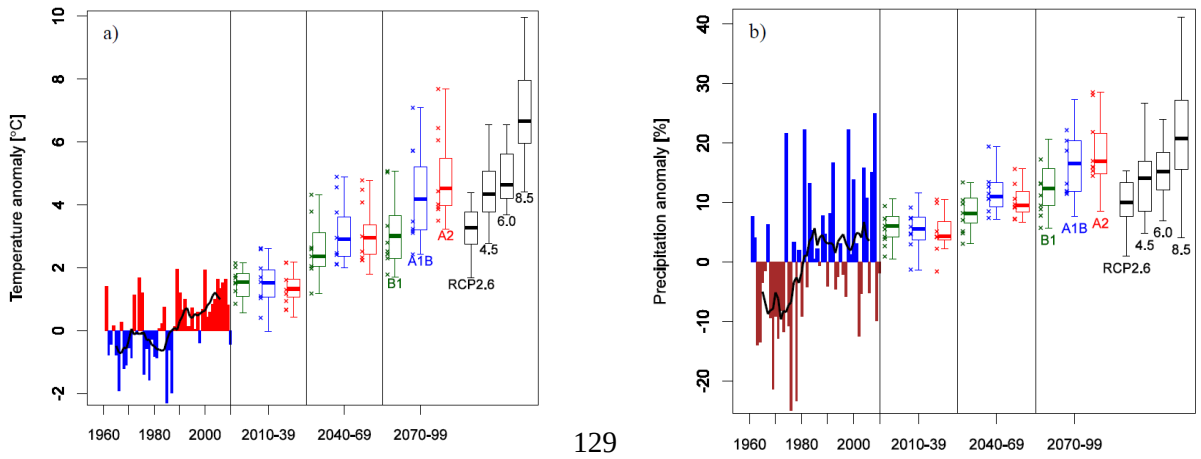

Figure 1. Observed anomalies in average annual (a) air temperature and (b) precipitation and projected changes for 30-year mean periods during the 21st century for Finland for SRES scenarios B1, A1B and A2 simulated with 8 GCMs selected for this study (stars) and for the full ensemble of 24 Coupled Model Intercomparison Project phase 3, CMIP3, models (boxplots), modified from Rötter et al. (2013). GCMs are listed in Table SA.1 in the supplementary material. Similar projected changes for RCP scenarios projected by CMIP5 GCMs are shown for last 30-year period.

The objective of this study was to predict gross primary production (*P*) and plant-water relations of boreal forests in Finland using climate scenarios for the 21st century from ensembles of GCMs with different forcings (both RCP and SRES). By showing both scenario families we acknowledge the fact that SRES scenarios are still used in impact studies, and even more so in policy analyses. Comparing the two sets of scenarios will help us put the SRES scenario results in perspective with those obtained from the RCP scenarios. We calculated *P* using a simple ecosystem flux model, PRELES, (Peltoniemi et al. 2015) with a generic boreal parameterisation (Minunno et al. 2016). We then quantified and compared the different sources of uncertainty, including the parametric uncertainty obtained from data-model assimilation, the structural uncertainty of C_a fertilization and water use effects, and input uncertainties originating in stochastic variability of weather and uncertainty created by the choice of climate model and forcing scenario. Using our study on GPP as an example, we discuss the implications more broadly in the framework of ecological impact model applications that are subject to large uncertainties.

2. MATERIALS & METHODS

2.1 The PRELES model

The PRELES model (Peltoniemi et al. 2015) describes *P* and water exchange (evapotranspiration, *E*) of forest canopies on the basis of light use efficiency (LUE), expressed as a multiplicative model of potential LUE and environmental modifiers f_i $(0 < f_i < 1)$. It inherits its photosynthesis part from Mäkelä et al. (2008) while a simple description of daily soil water balance was made in Peltoniemi et al. (2015). The model has been calibrated to eddy-covariance derived data on *P*, *E*, and measurements

of soil water in Scots pine stands (Peltoniemi et al. 2015), and a generic, species-independent parameterisation for boreal stands has been prepared (Minunno et al. 2016). While the existing model parameterisation has been carried out in current climate under constant C_a, here we extend the model to be applicable to future environment by incorporating an additional C_a modifier. Here we first outline the structure of the model, then introduce our treatment of the sources of mechanistic and input uncertainty. The details of PRELES are presented in Peltoniemi et al. (2015).

The photosynthetic production P (gC m^{-2} day^{-1}) is predicted in PRELES as:

$$P = f_{\mathrm{aPPFD}}\, P_0 \equiv \beta f_{\mathrm{aPPFD}} \sum_d \Phi_d \prod_i f_{id} \quad (1)$$

where f_{aPPFD} is the fraction of photosynthetic photon flux absorbed by the canopy, P_0 is the potential photosynthetic production when all radiation is absorbed ($f_{\mathrm{aPPFD}} = 1$), β is the potential light use efficiency (gC mol^{-1}, Table 1), Φ_d is photosynthetic photon flux density of day d (PPFD, mol m^{-2} day^{-1}), and f_{id} are values on day d of environmental modifiers related to variable i ($i = L, S, D, W$ representing light, temperature, vapour pressure deficit and soil water, respectively). The product of Φ and the light modifier f_L takes the form of rectangular hyperbola, which describes the saturating light effect on stand P, the temperature modifier f_S calculates the seasonal temperature potential for P. It is calculated using daily mean temperatures and over the course of the year the response typically takes a form resembling a cut sine wave where the peak values during summer are flattened to 1, while during the off-season (currently November-March in southern-most Finland) there is marginal or no potential to photosynthesize and its values are zero or close to zero. Impacts of the water vapor pressure deficit of atmosphere, D (VPD), and soil moisture, are implemented as $f_{D,W} = \min(f_D, f_{W,P})$. Here, f_D describes a modest exponential decrease of P with increasing D, and $f_{W,P}$ describes the decrease of photosynthesis with decreasing soil moisture content (Table 2 and Table 1 in appendix).

In order to calculate $f_{W,P}$, soil water balance and relative extractable water (W) are predicted using a simple bucket model where the water balance is controlled by precipitation, evapotranspiration, snowmelt, throughfall, and drainage. The modifier $f_{W,P}$ is then defined as $f_{W,P} = \min(1, W/\rho_P)$, i.e., low W below fitted parameter ρ_P thus potentially decreases $f_{D,W}$. The simple soil water model does not

describe lateral water flows, except that, above field capacity (θ_{FC}), a fraction of water is lost as runoff every day and becomes inaccessible to roots.

Evapotranspiration (E) is predicted using an empirical model, which is sensitive to P prediction, D, Φ, temperature, and f_{aPPFD}.

$$E = \alpha P f_{W,P}^{\nu} D^{1-\lambda} + \chi(1 - f_{aPPFD})\phi f_{W,E} \quad (2)$$

where parameters α, ν, λ and χ are fitted parameters, which partially determine the fraction of the two water fluxes (the two components of the sum, eq. 2) that correspond to transpiration and evaporation. The modifier $f_{W,P}$ of the P equation is raised to the power ν because P and E fluxes are not similarly influenced by drought. Modifier $f_{W,E}$ reduces evaporation under dry soil; formulation of $f_{W,E}$ modifier follows $f_{W,P}$ but has its own (fitted) threshold ρ_E, i.e. $f_{W,E} = \min(1, W/\rho_E)$. The model also includes a storage for surficial water (θ_{surf}) and snow (θ_{snow}), which are accounted for in the stand water balance. If $\theta_{surf} > 0$ or $\theta_{snow} > 0$ then $f_{W,E} = 1$.

For incorporating the CO_2 response in the model, the C_a effects on stand P were estimated using summary functions emulating the SPP stand photosynthesis model with Farquhar equations (Farquhar et al. 1980, Leuning 1995) for leaf photosynthesis (Mäkelä et al. 2006, Kolari et al. 2009). The SPP model simulations were done with using the SMEAR II stand as representative of typical middle-aged managed Scots pine stand (see Ilvesniemi et al. 2009 for detailed description of the site and stand structure).

The C_a influences both P and E through their own modifiers. The effects of soil moisture are partially influenced by C_a.

P is influenced by CO_2 of air in two ways. Firstly, if ambient CO_2 increases above its reference level $C_{a,ref}$, the photosynthetic efficiency will increase in a nonlinear manner which is described with the following modifier function:

$$f_{CO_2,P_0} = 1 + \frac{C_a - C_{a,ref}}{C_a - C_{a,ref} + C_{Sat}} \quad (3)$$

At the same time, however, the VPD response is also altered by decreasing the slope of the VPD response in increasing $C_a$due to partial closure of stomata, described as follows:

$$f_{CO2-D} = e^{\kappa_f \left(\frac{C_{a,re}}{C_a}\right)^{0.4} \cdot D} \quad (4)$$

Finally, the above reponses are combined in the following CO_2 modifier of photosynthesis:

$$f_{P,CO2} = f_{CO2,P0}\, f_{CO2\text{-}D} / f_D. \quad (5)$$

which describes the overall effect of C_a on photosynthesis.

The evapotranspiration, *E*, is also influenced by CO_2. Implementation of *E* changes under changed CO_2 concentration was made with a multiplier modifying the transpiration, i.e the first part of the model function for *E* (see Eqn 2 above):

$$f_{Tr,CO_2} = 1 - \frac{C_a - C_{a,ref}}{C_a - C_{a,ref} + C_{Sat}} \quad (6)$$

For more details, consult Mäkelä et al. (2008), Peltoniemi et al. (2015) and Minunno et al. (2016).

2.2 Standard set of model parameters

A standard set of parameters at reference C_a was obtained from the previous Scots pine stand parameterisation (Peltoniemi et al. 2015). The parameterisation under changing C_a was based on this reference case and the simulations of relative changes in the more detailed SPP model, as explained above (Table 1).

Tree species	Effective soil water holding capacity[§]	κ^{*}	$\beta^{‡}$	
Pine	167	0.13	0.75	Parameter set from Hyytiälä eddy-site that compared well with Sodankylä eddy-covariance site parameterization.
Spruce	210	0.4	0.75	
Birch	260	0.4	0.94	

§ The column height (mm) of extractable soil water roots of the trees have access to.

* Parameter of VPD sensitivity f-modifier, $f_D=e^{-\kappa D}$

‡ Deciduous species have clearly higher foliar [N] than conifers, which promotes higher β (Peltoniemi et al., 2012). Deciduous species LUE were predicted assuming a linear relationship between LUE and (Peltoniemi et al. 2012) mean needle N concentration (1.27 mgN $(gDM)^{-1}$ for pine and 2.40 mg $(gDM)^{-1}$ for birch, updated dataset of Merilä and Derome 2008). Mean pine needle N concentration in this dataset was assumed to generate the LUE estimated for Hyytiälä.

Table 1 Definition of tree species using model parameters. All other parameters were kept as defaults (Peltoniemi et al. 2015).

We further modified these pine (*Pinus sylvestris* L.) parameters on the basis of the literature (Mäkelä et al. 2008, Linkosalo et al. 2008, Minunno et al. 2016) to represent Norway spruce (*Picea abies* [L.] Karst.) and silver birch (*Betula pendula* Roth.) in the analysis (Table 1). In Minunno et al. (2016), the authors found no significant differences in the parameter estimates between Scots pine and Norway spruce dominated stands. Because spruce and birch generally occupy moister sites than pine, we increased the soil water holding capacity for them. The aim was to provide a realistic description of the typical growth sites of the different species. In addition, the parameter modifications assumed that spruce and birch had higher sensitivity to *D* than pine. Birch also has a higher light-use efficiency than pine and spruce (Peltoniemi et al. 2012). A description of the phenology of leaf budburst for birch was adopted from Linkosalo et al. (2008). This phenology model is an on-off variable which determines the date on which the temperature modifier f_S is activated. The phenology model does not account for

autumn phenology, i.e. there is no description of leaf-senescence and its potential effect on photosynthesis.

The fraction of absorbed photosynthetic photon flux density, f_{aPPFD}, essentially depends on forest structure. To screen the impact of structure on *P* we used three values (0.5, 0.75, and 1, Fig. SB.1 – SB.3), representing sparse, typical and theoretical stands that harvest different proportions of PPFD. The f_{aPPFD} also has a minor impact on the total amount of evapotranspiration and on the ratio of transpiration to evaporation.

2.3 Estimating PRELES parametric uncertainty

For estimating the parametric uncertainty of the impact model, we used a posterior distribution of parameters obtained with Bayesian inversion, and by applying the above adaptive Markov Chain Monte Carlo (MCMC) algorithm in the model calibration study (Peltoniemi et al. 2015). We used the differential evolution Markov chain (DEMC, ter Braak (2006)) algorithm to sample from the posterior distribution. The algorithm combines a global optimization algorithm, the differential evolution method of Storn and Price (1997), with an MCMC simulation step. A few Markov chains are run in parallel learning from each other. We used the DEMC version (ter Braak & Vrugt 2008) that uses a reduced number of chains (3) and a snooker updater implemented in the R package BayesianTools (Hartig et al., 2017). Here we varied 13 parameters of the posteriori (Table 2).

Parameter	Symbol	Unit	Used range
Potential light use efficiency	β_P	g C mol–1 m–2	0.685…0.810
Delay parameter for the response of temperature acclimation state to the changes in ambient temperature	τ	-	11.43…15.74
Threshold above which the state of acclimation increases	X_0	°C	-4.56…-2.97
Threshold at which the acclimation modifier reaches its maximum	S_{max}	$°C^{-1}\ d^{-1}$	17.75…20.08
Sensitivity parameter of *f*D to *D*	κ	kPa^{-1}	-0.196…-0.070
Light modifier parameter for saturation with irradiance	γ	$mol^{-1}\ m^{-2}$	0.029…0.041
Threshold for *W* effect on *P* in modifier *f*W,P	ρ_P	-	0.397…0.902
Transpiration parameter	α	mm (g C m–2 kPa1 – λ)–1	0.308…0.358

Parameter adjusting transpiration with *D*	λ	mol–1 m–2	0.100…0.919
Evaporation parameter	χ	mm mol–1	0.023…0.059
Threshold for *W* effect on evaporation in modifier *f*W,E	ρ_E	-	0.0002…0.9983
Parameter adjusting transpiration with *W*	ν	-	0.013…0.685
Surfacial water storage maximum	$\theta_{surf,max}$		0.422…5.000

Table 2. Parameters sampled from the posteriori of Peltoniemi et al. (2015) and their ranges used in the simulations.

We deemed 60 posteriori samples sufficient for characterizing the uncertainty of model parameters, their co-variation, consequent predictions of the model, as well as the distribution characterizing the distribution of residuals. The subset of the parameter vectors used in the simulations was sampled with even sized step from the posteriori distribution in such a manner that the whole parameter space formed by the posteriori was sampled. Figure SB.5 shows how the obtained subset covers the total variation of posteriori distribution of each parameter. The uncertainty of the mean response of the model (i.e. daily *P*) was generated using model parameters in the posterior sample. The uncertainty attributed to model parameters only partially captures the uncertainty of daily *P*. Around the mean response, there is variation of residuals, which stems from the uncertainties of observations used in the model calibration and inability of the model structure to describe the true variation. Therefore, for each day of the year in each simulated run, we drew a sample from the normal distribution with standard deviation *s*, centered on the simulated *P* for that day. Values of *s* were specific to the model parameters used; they were obtained from the same posterior sample as model parameters.

2.4 Structural uncertainty

The largest structural uncertainty of the model is related to the increased WUE due to C_a fertilization effect. The C_a effect was added to the model on the basis of a more detailed model (cf. Kolari et al.

2009), while the other environmental effects have been calibrated against data (Minunno et al. 2016). To quantify this uncertainty, we explored four alternative assumptions. Firstly, we assumed a full impact of the model described above, implying direct effects on photosynthesis and evapotranspiration and indirect effects on soil moisture through effects on evapotranspiration. Secondly, we assumed no effect on soil moisture, because it is possible that any reduction in transpiration due to C_a effects could be counteracted by increased evaporation (Allen et al. 2010). Thirdly, some studies have indicated a strong downregulation of photosynthesis even if C_a increases (Ellsworth et al. 2004); we therefore considered the possibility that C_a influences neither P nor evapotranspiration. Finally, we considered the hypothetical case that there was no effect of C_a on P and that soil moisture did not affect the processes at all. In this case, all effects are primarily caused by temperature increase.

These assumptions gave rise to the following model settings:

1. *All factors*

   The full model, including the effects of daily mean temperature (T, ºC), vapor pressure deficit (D, kPa), photosynthetic photon flux density above the canopy (ϕ, mol m^{-2}), C_a (ppm) and effective rooting zone soil water (θ, mm).

2. All factors less soil water: the case - *soil water*

   The effects of soil moisture constraint on P were removed, i.e. we set the soil water modifier in the model, $f_{W,P}$, to unity.

3. All factors less C_a: the case - C_a

   Here $C_a = C_{a,\,ref}$, which forces the $f_{P,CO2}$ and $f_{E,CO2}$ modifiers to 1.

4. All factors less soil water and C_a: the case - *CO_2 - soil water*

   Here $C_a = C_{a,\,ref}$, and constraints of soil moisture on P through soil water deficit were removed.

2.5 Input uncertainties: baseline and future climate data

Baseline daily weather data on a regular 10 km x 10 km grid covering Finland for the period 1971-2000 were obtained from the Finnish Meteorological Institute for mean temperature, precipitation, global

radiation and vapour pressure (Venäläinen et al. 2005). The estimation of PPFD and VPD from these data is described in Suppl. A. Climate scenarios for the 21st century were prepared by downscaling GCM simulations of the SRES emission scenarios (IPCC 2007) and the more recent Representative Concentration Pathways (RCPs, IPCC 2013) that took part in the Coupled Model Intercomparison Project (CMIP) phases 3 (for SRES, Meehl et al. 2007) and 5 (for RCP, Moss et al. 2010). Subsets of the full CMIP3 and CMIP5 ensembles were selected for which the required set of variables was available and which we regarded as representative for spanning the range of projected changes in the full ensembles. The criteria for representative ensembles were that they covered a sufficient range of uncertainty from a larger ensemble, and that the biases between the historical simulation and observed climate were not judged to be too large (Ruosteenoja 2011). For the SRES-based scenarios, eight GCM simulations of the B1, A1B and A2 emission scenarios were selected (cf. Figure 1 and Rötter et al. 2013). For RCP-based scenarios, 5 GCMs were selected, all covering the low RCP2.6, moderate RCP4.5 and high RCP8.5 forcing scenarios (Suppl. A Fig. SA.1, IPCC 2013).

Two alternative downscaling approaches were used: a simple change factor approach for the SRES simulations and bias-adjustment for the RCP simulations.

In the change factor approach, simulated monthly long-term changes in climate variables for the periods 2011-2040, 2041-2070 and 2071-2100 relative to 1971-2000 (Suppl. A Table SA.1) were used to adjust daily observed time series. The GCM grid cell centre point values were re-projected to the projection of the grid of the observed database and monthly changes were bi-linearly interpolated to estimate values for the centre points of the 10 x 10 km grid cells. For each grid cell, monthly changes were linearly interpolated to daily changes, which were added to the observed time-series. The development of C_a during 21st century was taken from simulations with the BERN carbon cycle model (Suppl. A Fig. SA.1, IPCC 2007). It is also assumed that the climate model bias remains the same in the simulations of future climate (Ruosteenoja et al. 2011). For further illustrations of the climate scenarios see Supplement A and details of the construction of climate scenarios see Rötter et al. (2013).

The dataset obtained from Finnish Meteorological Institute consisted of RCP-based simulations of climate input variables for the period 1980-2100. These data were bias-adjusted with observed daily data (Aalto et al. 2013) on a 10 x 10 km grid over Finland using quantile mapping (Suppl. A). The bias-adjusted model output was interpolated, using the bilinear method, onto a 10×10 km grid covering the area of Finland.

The bias-adjusted simulations represent a transient time-series from 1980 to 2100, whereas the SRES-based scenarios are not strictly a continuous, transient time-series, but 30-year time-series separate for baseline and three future periods.

2.6 Decomposition of sources of uncertainty

We estimated the uncertainty of GPP and ET projections arising from the impact model (parametric and structural uncertainty) and its weather inputs (scenario, climate model variation). The analysis was done separately for the RCP emission pathways and SRES emission scenarios.

We had $S = 3$ emission descriptions either in RCP (RCP2.6, RCP4.5 and RCP8.5) or SRES (A2, A1B, B1). For producing the climate projections we had an ensemble of $M = 5$ GCMs (CMIP5) for RCP and $M = 8$ GCMs (CMIP3) for SRES. We also included the parametric uncertainty of impact model ($K = 60$ parameter vectors). The parameter vectors were the same for both RCP and SRES analyses. For each year t we therefore calculated $S \times M \times K$ values of the predicted variable, i.e. annual mean GPP or ET value, denoted by x_{ksm}^{t}. The total variation could be described as a set of values, X^t, for each year:

$$X^t = \{x_{kms}^t \big| k = 1, \dots, K; m = 1, \dots, M; s = 1, \dots, S\} \quad (7)$$

Here *s* is either concentration pathway in RCP or SRES emission scenario, *m* is GCM, and *k* is parameter vector of PRELES. We then reduced the variation in three steps. First, we calculated the average over parameter vectors for each scenario and climate model and year, yielding values denoted by $x_{\cdot ms}^{t}$ and defining the set X_k^t:

373 $X_k^t := \{x_{ms}^t | m = 1, \dots, M; s = 1, \dots, S;\}$ (8)

374 The variability in X_k^t is therefore smaller than the overall variability, and the difference is accountable
375 to parameter uncertainty. Similarly, we averaged these over the GCMs, yielding

376 $X_{km}^t := \{x_{s}^t | s = 1, \dots, S\}$ (9)

377 The difference between X_{km}^t and X_k^t accounts for the GCM uncertainty. Finally, we defined the
378 following overall annual mean:

$$\hat{x}_t = \frac{1}{S} \times \frac{1}{M} \times \frac{1}{K} \sum_k \sum_m \sum_s x_{kms}^t \quad (10)$$

379 The variability around the mean created by X_{km}^t accounts for variability in concentration pathway /
380 emission scenario.

381 We then found minima and maxima in the sets X^t, X_k^t, and X_{km}^t for all years t. Combined with the
382 overall mean, this procedure gave us seven time series over the simulation period. We assumed that
383 these time series described the different components of variability in our predictions. We further fitted
384 smooth time functions to these discrete time series using linear functions or log-log transforms. For
385 estimating the natural variability of climate, we used the reference period (1980-2010) as a basis.

386

387 The above method for decomposing the uncertainty is descriptive and does not account for possible
388 interactions between the components. We therefore followed the approach of Nishina et al. (2015) and
389 carried out a three-way analysis of variance (ANOVA) for the annual GPP / ET for describing the
390 relative importance of the different sources of variation and their interactions as

391 $SS_{overall_t} = SS_{s_t} + SS_{m_t} + SS_{k_t} + SS_{s \times m_t} + SS_{s \times k_t} + SS_{m \times k_t} + SS_{s \times m \times k_t}$ (11)

392 in which *t* is year. $SS_{overall}$ is the total variability around the mean (sum of squares), and the other
393 symbols are as above. Here we also considered interaction effects between the components. We did
394 this analysis of decomposing uncertainty only for one grid point (10 km x 10 km) corresponding to the
395 location of Hyytiälä Forest station (southern Finland; 61°50.845N, 24°17.686E, 181 m a.s.l.).

396

397 ## 3. RESULTS

398

399 ### 3.1 Projections of GPP and ET for SRES-based climate scenarios

400 Climate change increased the species specific ensemble mean GPP in all simulation cases (cf. section
401 2.4) within all SRES scenarios and the magnitude of the changes followed the projected emissions in
402 the scenarios, being largest in A2 (in average 36%) and lowest in B1 (25%), while A1B was closer to
403 A2 (Fig. 2). The predicted GPP driven with projections of SRES and CMIP3 ensemble had a large
404 range which nearly corresponded to the change itself (relative range was 88% across scenarios at the
405 end of the period, Table 3). Considering the structural uncertainty, the C_a fertilization effect alone was
406 decisive for the overall impact on GPP in all species, regardless of what was assumed about soil
407 moisture (Fig. 2, Table 3).

408 If C_a fertilization effect was excluded (section 2.4, case 3.) and species pooled the average GPP increase
409 was almost the same in A2 (19%) and A1B (18%) and only slightly smaller in the B1 (14%) scenario.
410 Therefore, in B1 the ensemble range was much larger relative to the mean change itself (170%),
411 meaning that the most conservative climate change predictions yielded only conservative increases of
412 GPP by the end of the century.

413 Changes of other climatic factors, mostly temperature, also increased GPP in all scenarios (Fig. 2, black
414 filled circles). In the climate model projections with the largest increases in temperature, the effects of
415 other climatic factors roughly equalled those of C_a (Table 3). The minimum GPP estimates in B1
416 suggested that without the C_a effect, none of the species would benefit from climate change during the
417 first simulated period 2011-2040 (Fig. 2).

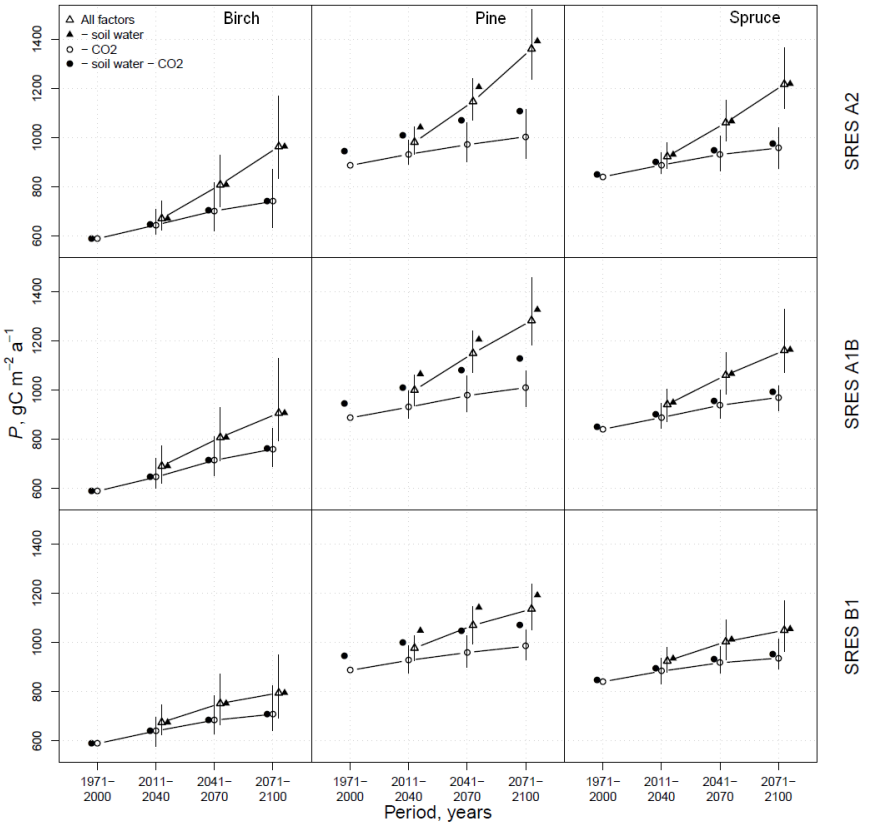

418

419 Figure 2. Effect of climate change on gross primary production (*P*) of forests in Finland with the
420 fraction of absorbed photosynthetic photon flux density (f_{aPPFD}) 0.75. Symbols show the mean
421 prediction obtained using the downscaled projections of eight CMIP3 global circulation models in
422 different SRES emission scenarios. Horizontal lines connect the symbols of "All factors" and "-CO_2"
423 simulation cases (see section 2.4). Vertical lines show the range of predictions obtained with these
424 projections (min – max), for clarity only for the same two simulation cases as in case of horizontal
425 lines.

426 Most of GPP increases can still be attributed to the increases of GPP in summer (May-Aug). Increases
427 of GPP in the winter-spring period (Jan-Apr) were approximately as high as increases of GPP in autumn
428 (Sep-Dec), suggesting that summer season radiation conditions dominate as drivers of annual GPP
429 increase (data not shown).

430 In the climate projections, the change in precipitation was less pronounced than change in e.g.
431 temperature (Fig. 1). Anyhow, the soil water constraint was relaxed due to decreasing transpiration in
432 the conifers (Fig. 3). This effect was clearest in pine which was the species most constrained by soil
433 water in reference climate due to low soil water holding capacity. This effect was only slight in spruce,

while birch GPP was not affected by soil moisture deficit in any of the time periods in any SRES emission scenario. When the C_a effect was excluded, the increased evapotranspiration exceeded the effect of larger rainfall and thus, GPP of pine was more constrained by soil water deficit in all SRES scenario climates than in the reference period (Fig. 3). In spruce this effect was much less pronounced and in birch it could not be detected.

Species	Scen	Case	Period	Mean	Max	Min	Relative		
							Mean	Max	Min
Birch	B1	All_factors	2011-2040	676	748	625	0.17	0.30	0.09
			2041-2070	752	873	665	0.31	0.52	0.16
			2071-2100	795	948	694	0.38	0.65	0.21
		No_CO2	2011-2040	641	696	576	0.09	0.18	-0.02
			2041-2070	685	785	630	0.16	0.33	0.07
			2071-2100	709	826	643	0.20	0.40	0.09
	A1B	All_factors	2011-2040	691	773	621	0.20	0.34	0.08
			2041-2070	807	930	714	0.40	0.62	0.24
			2071-2100	907	1129	795	0.58	0.96	0.38
		No_CO2	2011-2040	646	723	602	0.10	0.23	0.02
			2041-2070	715	809	651	0.21	0.37	0.10
			2071-2100	760	846	687	0.29	0.44	0.17
	A2	All_factors	2011-2040	671	741	623	0.17	0.29	0.08
			2041-2070	808	930	718	0.41	0.62	0.25
			2071-2100	964	1168	834	0.68	1.03	0.45
		No_CO2	2011-2040	645	710	608	0.09	0.21	0.03
			2041-2070	702	817	622	0.19	0.39	0.06
			2071-2100	741	871	634	0.26	0.48	0.08
Spruce	B1	All_factors	2011-2040	925	979	880	0.13	0.20	0.07
			2041-2070	1003	1094	931	0.22	0.34	0.14
			2071-2100	1050	1169	964	0.28	0.43	0.18
		No_CO2	2011-2040	884	935	831	0.05	0.11	-0.01
			2041-2070	918	984	876	0.09	0.17	0.04
			2071-2100	937	1013	891	0.11	0.21	0.06
	A1B	All_factors	2011-2040	941	1002	873	0.15	0.22	0.07
			2041-2070	1060	1154	984	0.29	0.41	0.20
			2071-2100	1161	1328	1072	0.42	0.62	0.31
		No_CO2	2011-2040	888	948	844	0.06	0.13	0.00
			2041-2070	938	1002	886	0.12	0.19	0.05
			2071-2100	970	1016	915	0.15	0.21	0.09
	A2	All_factors	2011-2040	923	981	875	0.13	0.20	0.07
			2041-2070	1061	1153	985	0.29	0.41	0.20
			2071-2100	1217	1366	1117	0.49	0.67	0.36
		No_CO2	2011-2040	888	937	854	0.06	0.12	0.02
			2041-2070	931	1008	865	0.11	0.20	0.03
			2071-2100	958	1042	875	0.14	0.24	0.04
Pine	B1	All_factors	2011-2040	977	1027	926	0.14	0.20	0.08
			2041-2070	1070	1146	996	0.25	0.34	0.16
			2071-2100	1136	1238	1052	0.33	0.45	0.23
		No_CO2	2011-2040	928	986	874	0.05	0.11	-0.01
			2041-2070	959	1029	898	0.08	0.16	0.01
			2071-2100	985	1052	928	0.11	0.19	0.05
	A1B	All_factors	2011-2040	1000	1061	935	0.17	0.24	0.09
			2041-2070	1150	1242	1070	0.34	0.45	0.25
			2071-2100	1283	1458	1184	0.50	0.70	0.38
		No_CO2	2011-2040	931	999	886	0.05	0.13	0.00
			2041-2070	977	1057	913	0.10	0.19	0.03
			2071-2100	1010	1080	931	0.14	0.22	0.05
	A2	All_factors	2011-2040	981	1044	932	0.15	0.22	0.09
			2041-2070	1147	1239	1070	0.34	0.45	0.25
			2071-2100	1361	1520	1238	0.59	0.78	0.45
		No_CO2	2011-2040	932	989	890	0.05	0.12	0.00
			2041-2070	971	1059	902	0.10	0.19	0.02
			2071-2100	1004	1115	915	0.13	0.26	0.03

Table 3 Changes of gross primary production (P, g C m^{-2} a^{-1}) with default parameter set of PRELES and the downscaled projections of the ensemble of eight CMIP3 -GCMs over Finland separately in SRES B1, A1B and A2 scenario with the fraction of absorbed photosynthetic photon flux density (f_{aPPFD}) 0.75.

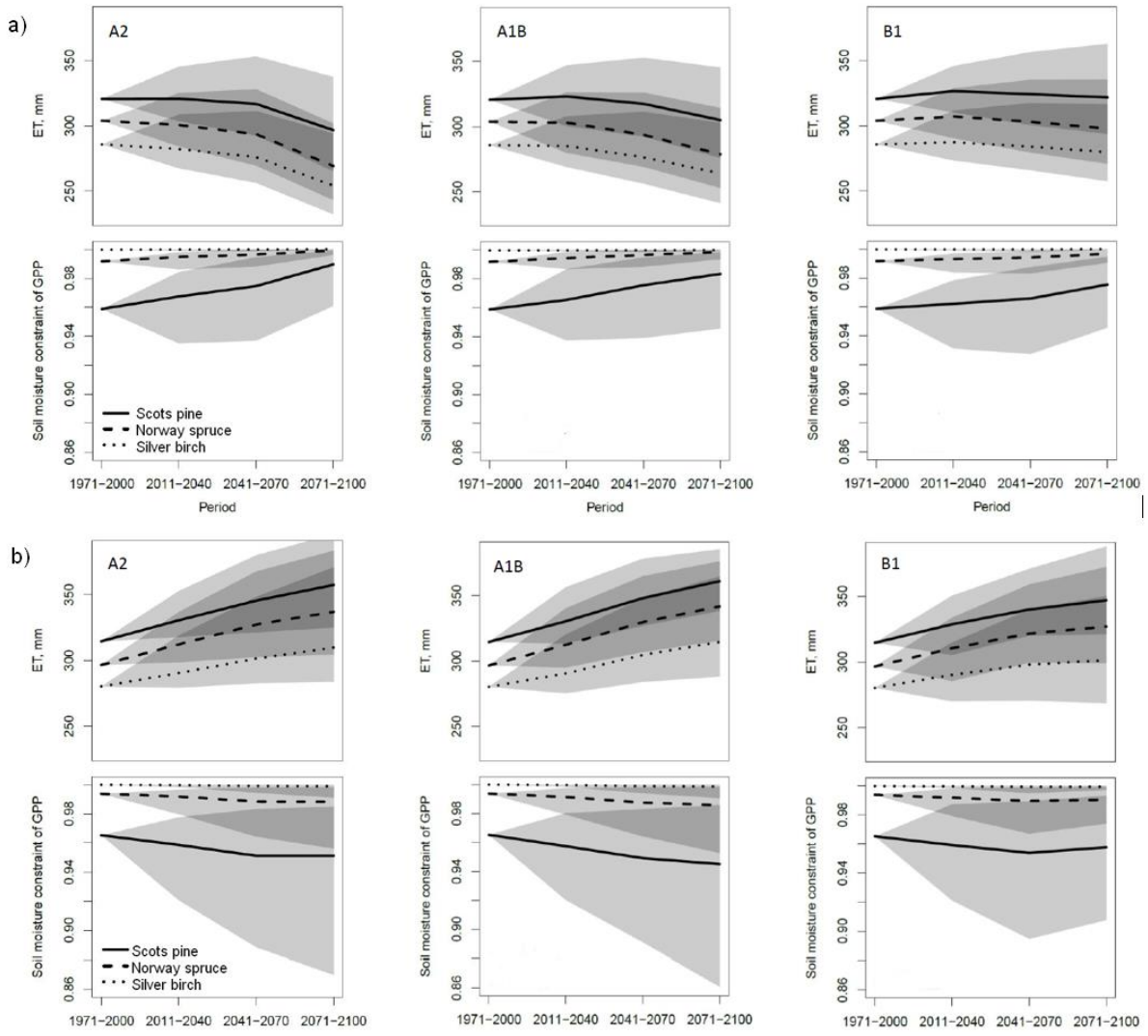

Figure 3. Simulated evapotranspiration E and soil moisture constraint in SRES scenarios during 21st century in simulation cases A) '*All factors*' and B) '*All factors less* C_a'. The gray-shaded bands are the range of the response variable obtained with the downscaled projections ofeight CMIP3 GCMs in different SRES scenarios.

453 The increase of GPP was in absolute terms only slightly larger in southern than in northern Finland in
454 all simulated SRES cases. Relative increases were thus higher in the north in all modelled species and
455 the range of GPP predictions was also larger in northern than in southern Finland (Fig. 4).

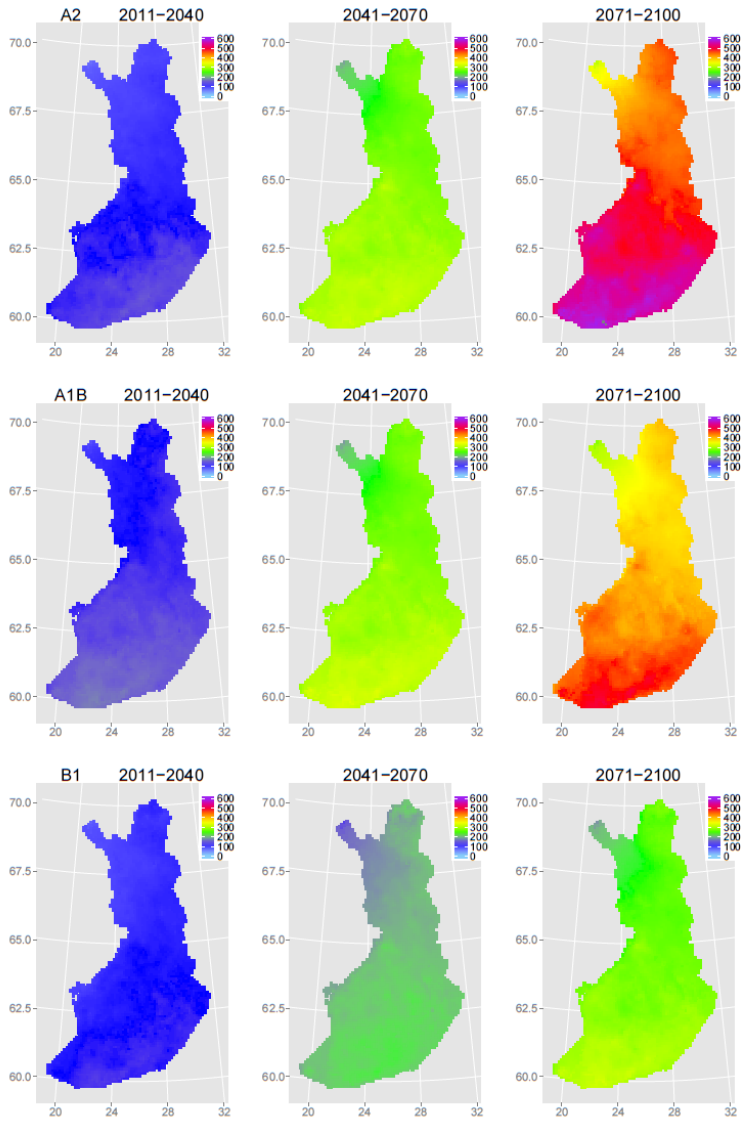

456

457 Figure 4. The range of change of gross primary production (*P*, g C m^{-2}) predictions for Scots pine in
458 simulation case '*All factors*' with the downscaled projections of the ensemble of eight CMIP3 8-
459 GCMs and with faPPFD = 0.75 in the different SRES emission scenarios.

460

461 The relative change in GPP was the highest in birch in North Finland, up to 80% (44% – 127%) in the
462 A2 scenario at the end of the century (Table 3). Larger increases of GPP in birch than in other species
463 were predominantly caused by a stronger effect of the temperature increases. This was illuminated by

464 the result that when C_a fertilization effect (case 3.) was excluded the changes were still the most
465 pronounced for birch, 33% (7% – 69%, Table 3).
466
467 **3.2 Contribution of different uncertainty sources to GPP and ET**
468 In absolute terms, the overall uncertainty increased greatly over time both in GPP and ET and differed
469 clearly between SRES and RCP simulations (Fig. 5, Fig. SA.5). However, the pattern of the GPP in
470 terms of the fraction of uncertainty for each variable was quite similar in both (Fig. 6). The year to year
471 variation was large being ca. 55% in SRES and 48% in RCP and could be detected even in smoothed
472 five years average (Fig. 6). The relative importance of the different sources of uncertainty changed over
473 time in both the predictions of GPP and ET. For GPP, the GCM uncertainty dominated roughly before
474 2060 and emission uncertainty thereafter. For ET, GCM uncertainty remained the largest throughout
475 21st century in SRES while RCP emission uncertainty exceeded that of GCMs only around 2080. In
476 GPP of the SRES, the emission uncertainty never exceeded the natural variability while in RCP this
477 occurred already around 2060 (Fig. 5). A significant interaction effect between emission scenario
478 uncertainty and GCM uncertainty was found for SRES but not for RCP. The uncertainty due to PRELES
479 parameters was almost negligible in predictions of GPP but much larger in the predictions of ET in both
480 SRES scenarios and RCP pathways. In ET also, the dominant role of variation between GCMs was
481 eminent (Fig. 6).

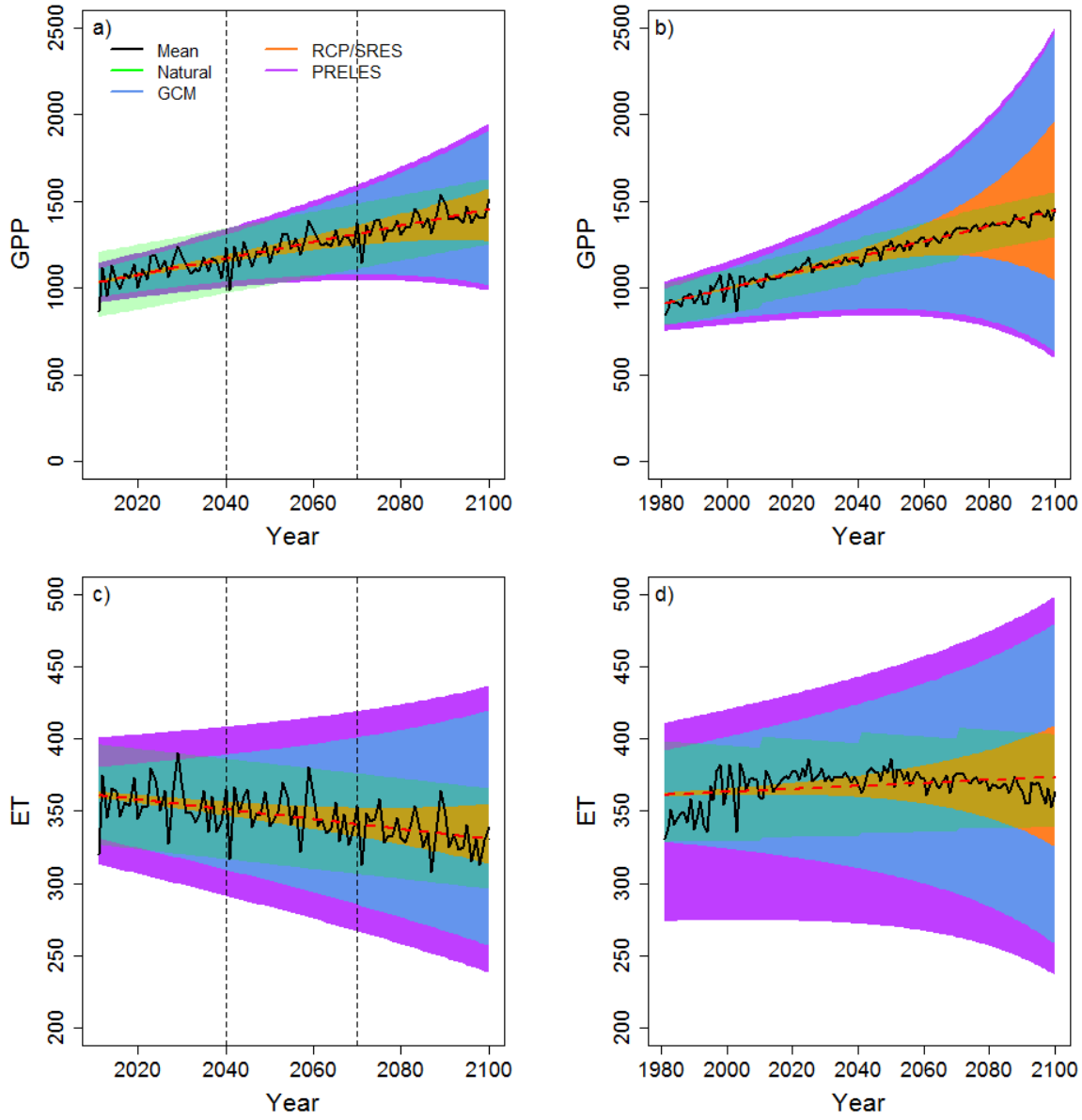

Figure 5. Role of different sources of uncertainty (see eqs. 7-10) on the predicted Scots pine GPP and ET in one grid cell (Hyytiälä Forest Station). The different colors are additive and total uncertainty ($S \times M \times K$) is illustrated by total colored area. The colors indicate removing one source of uncertainties stepwise, starting from PRELES parametric and structural uncertainty (purple area, $K = 60$ parameter vectors, same vectors for both RCP and SRES), GCM variability (blue area, $M = 5$ CMIP5 GCMs for RCP and $M = 8$ CMIP3 GCMs for SRES), and emission pathways/scenarios (orange area, $S = 3$ emission descriptions separately for RCP [RCP2.6, RCP4.5, RCP8.5], and SRES [A2, A1B, B1]). The lighter color in the middle indicates the natural climatic variability. a) GPP in SRES, b) GPP in RCP, c) ET in SRES, d) ET in RCP. The vertical dashed lines illustrate the climate periods used in SRES (1980-2010, 2011-2040, and 2041-2100). In RCPs, transient climate data were used (1980-2100).

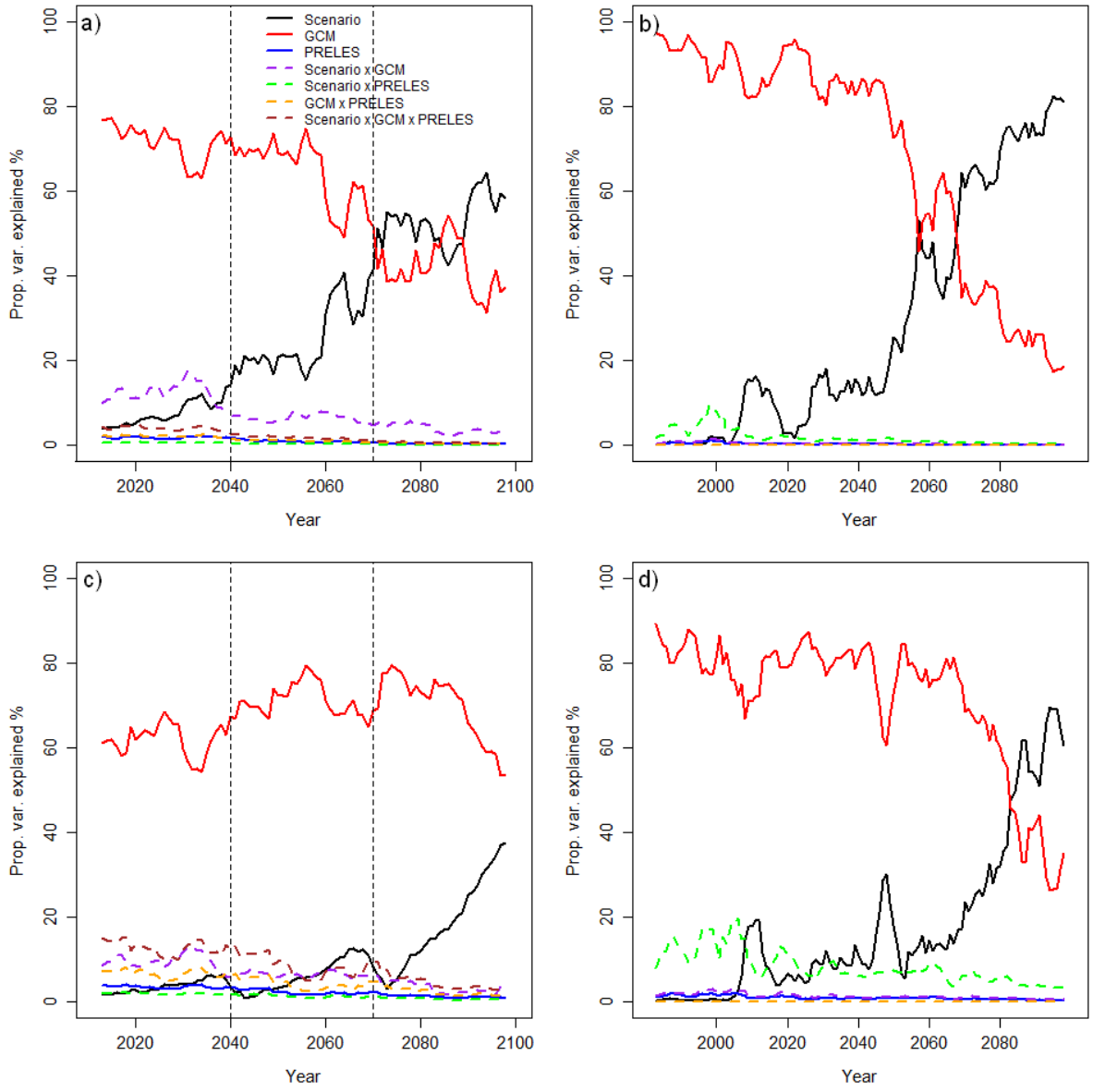

Figure 6. ANOVA (see eq. 11) for Scots pine GPP and ET in one grid cell (Hyytiälä Forest Station) separately for RCP [RCP2.6, RCP4.5, RCP8.5], and SRES [A2, A1B, B1]). a) GPP in SRES b) GPP in RCP, c) ET in SRES and d) ET in RCP. The vertical dashed lines illustrate the climate periods used in SRES (1980-2010, 2011-2040, and 2041-2100). In RCPs, transient climate data were used (1980-2100).

4. DISCUSSION

The starting point for any model based analysis of the carbon cycles is the reliable description of gross primary production. We covered a broad envelope of predictions, multiple GCMs and multiple emission scenarios with one impact model, allowing us to make conclusions on the types of change that seem

likely for different species or sites. Moreover, our results revealed the sensitivity of predictions of the PRELES model to input uncertainty and how the variability of GPP and ET propagates from emissions scenarios to the assumptions of the impact model CO_2 response function. The most general finding was that the selection of the climate change projection had a profound influence on both the predicted GPP and ET of boreal forests of Finland. Many studies concerning different ecological impacts of climate change, e.g. disturbances (e.g. Lehtonen etal. 2016, Seidl et al. 2017) have noted this. We considered here a continuous variable whereas disturbance is always discrete which emphasizes the need for specific analysis for different impacts. However, in both cases the wide range of projections may lead to difficulties in drawing ecologically meaningful conclusions (Cavanagh et al. 2017). Real uncertainty is even larger due to feedback loops between climate and vegetation (e.g. Forzieri et al. 2017) which we could not account for with a simple tool like PRELES.

The highest predictions of GPP were almost double compared with present day observations, while the lowest predictions without C_a fertilization effect did not increase GPP during the next decades and barely during the whole century. The species specific mean GPP increased in all simulated cases and was generally in the same scale as found in earlier studies with more mechanistic models (Wamelink et al. 2009, Ge et al. 2013, Reyer et al. 2014). Our finding that the decomposition of uncertainty hardly differed between combinations of older SRES emission scenarios and CMIP3 projections and the currently used RCPs and CMIP5 GCMs lends support to the robustness of this result. The difference of the climate projections for Finland between SRES and RCP scenarios seems to be quite modest (Fig. 1) especially if compared with the high variability between projections of individual GCMs (Fig 6). Thus, from the viewpoint of forest impact studies SRES and RCP projections essentially cover the same range (van Vuuren and Carter 2014). Our results were consistent with earlier studies in the sense that GCMs were the dominant sources of uncertainty for GPP until around 2060, while uncertainty of the temporal development of emissions, either driven by RCP or SRES scenarios, dominated later in the projection period (2060–2100, Nishina et al. 2015, Horemans et al. 2016). We note that this uncertainty analysis only covered one grid point (Hyytiälä forest station), but extending it to the whole country

would likely not create more than marginal changes to the decomposition of uncertainty, due to the small parametric variation in PRELES.

The difference of variation between RCP and SRES observed here was partly due to the fact that selected pathways of RCPs were more extreme than emission scenarios of SRES (RCP2.6 vs SRESB1 and RCP8.5 vs SRESA2). In addition, GCMs have developed from CMIP3 to CMIP5. However, although characteristics of the CMIP5 models have changed from CMIP3, e.g. they may have higher resolution, their atmospheric or ocean components may have changed in order to improve their ability to describe the fluxes between ecosystems and the atmosphere, the models in the new ensemble are neither independent of each other nor independent of the earlier generation (Knutti et al. 2013). From the impact viewpoint, one could thus argue that the characteristics of input uncertainty have not changed that much between these two generations of GCMs. Additional variability between RCP and SRES in our analysis was created by the fact that we did not have the same GCMs in the compiled subset of projections (see Suppl. A), and that the method for downscaling the results of GCMs for Finland differed between RCP and SRES. In SRES thirty-year periods of historical data were coupled with GCM projections to produce the climate for the whole century, while in the case of RCPs, the GCM projections directly provided the transient climate change from 1980 to 2100. This contributed to fairly different natural variability between RCP and SRES (Fig. 6, Suppl. A).

The dominant role of GCM over emission scenario as a driver of uncertainty of the impact studies outcome has not been pointed out in earlier Finnish studies (e.g. Kellomäki et al. 2008. Ge et al. 2013). In boreal-forest related studies this is of special importance due to the fact that the time perspective of tree growth approaches that of climate change. Our results demonstrate that impact studies with a single GCM projection may not expose the full range of possible changes and thus, may lack information about local/regional scale impacts that would be essential for decision making (e.g. Lung et al. 2013). Our understanding is that forest related climate mitigation policies do pose a risk that actions are based on mean response not on the range of scenarios, the relative probabilities of which cannot be specified

559 at this point of time. It would therefore be extremely helpful for coherent decision-making if reporting
560 overall uncertainty and its component sources was standard practise in scientific impact studies.
561
562 Structural uncertainty of the model, i.e., uncertainty due to our deficient scientific understanding of the
563 process at hand, was represented here by the response of gas exchange to long-term CO_2 fertilization.
564 Under the default assumptions, the direct influence of C_a on GPP (species pooled) was 50% of the total
565 impact in A2 scenario and roughly 40% in A1B scenario and up to 38% in B1 at the end of the century,
566 but the increase was sensitive to assumptions of C_a effects on WUE. Severe production limitations due
567 to soil moisture availability seem unlikely if transpiration of trees is moderated by increased C_a. Without
568 the assumptions of C_a-induced reductions of transpiration, there would be more sites suffering from
569 drought in the future (Fig. 3b). Relative humidity (RH%) has been found to be a critical factor to
570 differentiate the projected NPP among different Global Vegetation Models (Nishina et al. 2015). We
571 derived vapor pressure deficit (*D*) using RH% predicted by the GCMs, while earlier Finnish studies
572 have assumed unchanged RH% of air (e.g. Kellomäki et al. 2008, Ge et al. 2013), but both approaches
573 lead to increased *D*. Earlier research concerning Finland has warned about vulnerability to climate
574 change of spruce growing on dry sites. However, based on our study, a crucial aspect for species
575 management is that, species responsive to *D* and occupying moist sites will perform well. Drought-
576 vulnerable sandy dry or uphill sites (Muukkonen et al. 2015) tend to be Scots-pine dominated already
577 in the current climate. The species-specific responses of our study must be interpreted with caution, as
578 the parameter adjustments were made subjectively on the basis of available but insufficient information.
579 Concerning conclusions of these water effects, one has to keep in mind the weak ability of GCMs to
580 represent within-year, seasonal and day-to-day variability of weather. This issue is the most critical one
581 for rainfall since rains could become more sporadic and intense in the northern hemisphere (e.g. Jylhä
582 et al. 2009, Rummukainen 2012, 2013), with possibility off increased frequency of longer periods of
583 drought. Neither we nor earlier studies accounted for this specific property of input uncertainty.
584

585 The applied PRELES model has been parameterized with several years of eddy-covariance data
586 including considerable within-year variability of fluxes. We have found that the model also performs
587 well at warmer and colder eddy-covariance sites (Minunno et al 2016). Further support for plausible *P*
588 predictions has been obtained through a comparison with the JSBACH model (Reick et al. 2013) at the
589 scale of Finland (Peltoniemi et al. 2015). In this study, we found that the proportion of PRELES
590 parametric uncertainty from total uncertainty was almost marginal in the projections of GPP. This
591 indicates that lots of data were used in the calibration and the most important parameters were well
592 constrained. We acknowledge that under the changing environmental conditions we were not able to
593 fully separate model structural uncertainty from the parametric uncertainty but PRELES uncertainty
594 here only describes the variability included in the calibration dataset (Minunno et al. 2016) and, thus,
595 did not increase over time. This is a general challenge in calibration, especially in the case of simple
596 models. It could be that processes not important in the current environment become major issues in the
597 future, and thus the impact model uncertainty is not reflected coherently. One way forward could be to
598 test PRELES with different CO_2 response functions against data from FACE experiments, and/or to
599 calibrate the functions in such data sets. This could be very informative bearing in mind that the
600 structural uncertainty related to this driver had a prominent effect on the model predictions. Our results
601 also do not account for the possible increase in canopy size as a result of increasing GPP which could
602 also lead to increasing ET and hence more pronounced drought effects, however, a comparison of
603 simulations with different f_{aPPFD} values may provide a cue. In our simulations increasing f_{aPPFD} from
604 0.75 to 1 had an effect on *E* comparable to the (opposite) C_a-induced reduction of transpiration (Fig.
605 SB2).
606
607 There are numerous effects we did not consider in our analysis. Restriction of tree response due to soil
608 nitrogen limitation may downregulate the CO_2 fertilization effect. Long-term growth stimulation has
609 been found only under high nutrition (e.g. fertilized sites or on former agricultural land) or explained
610 as a result of priming effects (see references in Palacio et al. 2014). The main effects of nutrients
611 (particularly nitrogen as the main limiting nutrient in boreal forest) are (1) increased photosynthetic
612 capacity of foliage (Reich et al. 1998, Peltoniemi et al. 2012), and (2) increased carrying capacity, i.e.,

613 the total foliage that can be supported by the stand (Ladanai and Ågren 2004, Mäkelä et al. 2008). In
614 boreal conifers the increased photosynthetic capacity due to variation in foliar N concentration is
615 relatively modest (e.g. Peltoniemi et al. 2012), whereas the impacts of changes in carrying capacity
616 could be considerable. The effects of increasing canopy cover and consequently f_{aPPFD} were already
617 discussed above. However, whether or not the canopy cover will increase under climate change also
618 depends on the response of nutrient availability to climate, as the increased CO_2 fertilisation is known
619 to strengthen the carbon sink below ground under N limitation (Norby et al. 2010). Here, more
620 information is needed on trends in N deposition, implications of the priming effect, as well as impacts
621 of weather drivers on soil organic matter decomposition. In order to account for the nutrient cycle
622 which could either up- or down-regulate the predicted increases in GPP, e.g. nitrogen modifier could
623 be included in PRELES based on approaches like Peltoniemi et al. (2012). We also did not include any
624 nitrogen deposition scenario. However, nitrogen deposition does not play a big role in Finland when
625 compared with e.g. Central Europe. Also the effect of climate extremes and especially their connection
626 to the changing disturbance regimes we did not include in the predictions. When considering the carbon
627 cycling the increasing disturbances may have a much bigger role in the future than in current conditions
628 (Seidl et al. 2017). All these additional effects will further increase the uncertainty of GPP projections
629 into the future.
630

631 ## 5. CONCLUSIONS

632 We consider it very likely that primary production of Finnish forests will be higher in the future than it
633 is now. However, uncertainty around this mean response is very large and our decomposition of its
634 sources demonstrates that more constraining information is needed equally on the biological
635 mechanisms and on the expected environmental drivers before the projections can be made more
636 conclusive. Regarding the mechanisms, we need to improve our scientific understanding of the
637 interactions of CO_2 fertilization with water and nutrient fluxes (Figs. 2 and 3). At the same time, our
638 analysis underlines the need of transparency in modelling studies about how input uncertainty from
639 emission scenarios and different GCMs and their assumptions propagates to ecological impacts (Figs.

5 and 6). Transparency is easier to reach if the modelling approach is relatively simple, such as in the present study. It is encouraging in this respect that our results were much in line with previous studies obtained with highly mechanistic, complex models. We believe that these general methodological conclusions can be extended to more comprehensive models, such as models of the full vegetation carbon budget, although our example model only considered gross primary production.

Acknowledgements We thank Pasi Kolari for the CO_2 modifier in PRELES model. We gratefully acknowledge the contribution of the Academy of Finland project CARB-ARC (No. 286190) and LIFE+ financial instrument of the European Union (LIFE12 ENV/FI/000409 Monimet, http://monimet.fmi.fi).

The work was made in the frame of COST Action FP1304 PROFOUND.

Appendix List of the variables and functions of PRELES model.

Variable (model input or estimated by the model)	Symbol	Unit
Daily precipitation (water or snow)	R	mm
Drainage	F	mm
Drainage from surfacial water storage to soil (after $\theta_{surf,max}$ is reached)	F_{surf}	mm
Evapotranspiration from snow storage	E^{snow}	mm
Evapotranspiration from soil storage	E^{soil}	mm
Evapotranspiration from surficial water storage	E^{surf}	mm
Fraction of absorbed photosynthetic photon flux density	f_{aPPFD}	–
Gross primary production	P	gCm^{-2}
Leaf area index	L_A	–
Light modifier	f_L	–
Minimum of vapour pressure deficit and soil water modifier	$f_{DW,P}$	–
Modifier for temperature acclimation state, cf. S	f_S	–
Photosynthetic photon flux density	Φ	mol^{-1} m^{-2}
Rainfall, as rain	R^1	mm
Relative extractable water	W	–
Soil water modifier for evaporation	$f_{W,E}$	–
Snow/ice water content (in water equivalents)	θ_{snow}	mm
Snowfall	R^0	mm
Snowmelt	M	mm
Soil water content	θ	mm
Soil water modifier for gross primary production	$f_{W,P}$	–
State of acclimation to temperature	S	°C
Surfacial water content, e.g. on leaf and soil surfaces (has an upper limit defined by subscript 'max')	θ_{surf}	mm
Temperature, daily mean	T	°C
Vapour pressure deficit, daily mean	D	kPA
Vapour pressure deficit modifier	f_D	–

6. REFERENCES

Aalto J, Pirinen P, Heikkinen J, Venäläinen A (2013) Spatial interpolation of monthly climate data for Finland: comparing the performance of kriging and generalized additive models. Theor Appl Climatol 112:99–111

Ahlström A, Schurgers G, Arnet A and Smith B (2012) Robustness and uncertainty in terrestrial ecosystem carbon response to CMIP5 climate change projections. Env Res Let 7:1-9

Ainsworth EA, Rogers A (2007) The response of photosynthesis and stomatal conductance to rising [CO2]: mechanisms and environmental interactions. Plant Cell Env 30:258-270

Allen CD, Macalady AK, Chenchouni H, Bachelet D, McDowell N, Vennetier M, Kitzberger T, Rigling A, Breshears DD, Hogg EH(T.), Gonzalez P, Fensham R, Zhang Z, Castro J, Demidova N, Lim J-H, Allard G, Running SW, Semerci A, Cobb N. A global overview of drought and heat-induced tree mortality reveals emerging climate change risks for forests. For Ecol Manage 259:660-684.

Bergh J, Freeman M, Sigurdsson B, Kellomäki S, Laitinen K, Niinistö S, Peltola H, Linder S (2003) Modelling the short-term effects of climate change on the productivity of selected tree species in Nordic countries. For Ecol Manage 183:327-340

Bonan GB (2008) Forests and climate change: forcings, feedbacks, and the climate benefits of forests. Science 320:1444-1449

Rachel D. Cavanagh1*, Eugene J. Murphy1, Thomas J. Bracegirdle1, John Turner1, Cheryl A. Knowland1†, Stuart P. Corney2, Walker O. Smith, Jr.3, Claire M. Waluda1, Nadine M. Johnston1, Richard G. J. Bellerby4,5, Andrew J. Constable2,6, Daniel P. Costa7, Eileen E. Hofmann8, Jennifer A. Jackson1, Iain J. Staniland1, Dieter Wolf-Gladrow9 and José C. Xavier1,10 (2017) A Synergistic Approach for Evaluating Climate Model Output for Ecological Applications

De Kauwe MG, Medlyn BE, Zaehle S, Walker AP, Dietze MC, Hickler T, Jain AK, Luo Y, Parton WJ, Prentice IC, Smith B, Thornton PE, Wang S, Wang Y, Wårlind D, Weng E, Crous KY, Ellsworth DS, Hanson PJ, Seok Kim H, Warren JM, Oren R, Norby RJ (2013) Forest water use and water use efficiency at elevated CO2: a model-data intercomparison at two contrasting temperate forest FACE sites. Glob Change Biol 19:1759-1779

Dewar RC, Medlyn BE, McMurtrie RE (1998) A mechanistic analysis of light and carbon use efficiencies. Plant Cell Env 21:573-588.

Ellsworth DS, Reich PB, Naumburg SE, Koch GW, Kubiske ME, Smith SD (2004) Photosynthesis, carboxylation and leaf nitrogen responses of 16 species to elevated pCO2 across four free-air CO2 enrichment experiments in forest, grassland and desert. Glob Change Biol 10:2121-2138.

Farquhar GD, Caemmerer S, Berry J (1980) A biochemical model of photosynthetic CO_2 assimilation in leaves of C3 species. Planta 149:78-90.

Forzieri G, Alkama R, Miralles DG, Cescatti A (2017) Satellites reveal contrasting responses of regional climate to the widespread greening of Earth. Science 356:1180-1184.

Ge Z, Kellomäki S, Peltola H, Zhou X, Väisänen H, Strandman H (2013) Impacts of climate change on primary production and carbon sequestration of boreal Norway spruce forests: Finland as a model. Clim Change 118:259-273

Hartig F, Minunno F, Paul S (2017) BayesianTools: General-Purpose MCMC and SMC Samplers and Tools for Bayesian Statistics. R package version. R package version 0.0.0.9000. <https://cran.r-project.org/web/packages/BayesianTools/index.html>.

Horemans JA, Bosela M, Dobor L, Barna M, Bahyl J, Deckmyn G, Fabrika M, Sedmak R, Ceulemans R (2016) Variance decomposition of predictions of stem biomass increment for European beech: Contribution of selected sources of uncertainty. For Ecol Manage 361:46-55.

IPCC (2007) Climate Change 2007: The Physical Science Basis. Contribution of Working Group I to the Fourth Assessment Report of the Intergovernmental Panel on Climate Change. Cambridge University Press, Cambridge, United Kingdom and New York, NY, USA

IPCC, 2013: Climate Change 2013: The Physical Science Basis. Contribution of Working Group I to the Fifth Assessment Report of the Intergovernmental Panel on Climate Change [Stocker, T.F., D. Qin, G.-K. Plattner, M. Tignor, S.K. Allen, J. Boschung, A. Nauels, Y. Xia, V. Bex and P.M. Midgley (eds.)]. Cambridge University Press, Cambridge, United Kingdom and New York, NY, USA, 1535 pp, doi:10.1017/CBO9781107415324.

Jylhä K, Ruosteenoja K, Räisänen J, Venäläinen A, Tuomenvirta H, Ruokolainen L, Saku S, Seitola T (2009) The changing climate in Finland: estimates for adaptation studies. ACCLIM project report 2009. Finn Meteorol Inst.Reports 4

Keenan TF, Hollinger DY, Bohrer G, Dragoni D, Munger JW, Schmid HP, Richardson AD (2013) Increase in forest water-use efficiency as atmospheric carbon dioxide concentrations rise. Nature 499:324-327

Kellomäki S, Peltola H, Nuutinen T, Korhonen KT, Strandman H (2008) Sensitivity of managed boreal forests in Finland to climate change, with implications for adaptive management. Philos Trans R Soc B: Biological Sciences 363:2339-2349

Knutti R, Masson D, Gettelman A (2013) Climate model genealogy: Generation CMIP5 and how we got there. Geophys Res Lett 40:1194-1199.

Kolari P, Kulmala L, Pumpanen J, Launiainen S, Ilvesniemi H, Hari P, Nikinmaa E (2009) CO_2 exchange and component CO_2 fluxes of a boreal Scots pine forest. Bor Env Res 14:761-783

Ladanai S, Ågren GI (2004) Temperature sensitivity of nitrogen productivity for Scots pine and Norway spruce. Trees 18:312-319

Lehtonen I, Venäläinen A, Kämäräinen M, Peltola H, Gregow H (2016) Risk of large-scale fires in boreal forests of Finland under changing climate. Nat Hazards Earth Syst Sci 16:239-253.

Leuning R (1995) A critical appraisal of a combined stomatal-photosynthesis model for C3 plants. Plant Cell Env 18:339-355

Linkosalo T, Lappalainen HK, Hari P (2008) A comparison of phenological models of leaf bud burst and flowering of boreal trees using independent observations. Tree Physiol 28:1873-1882

763 Liski J, Lehtonen A, Palosuo T, Peltoniemi M, Eggers T, Muukkonen P, Mäkipää R (2006) Carbon
764 accumulation in Finland's forests 1922-2004 - and estimate obtained by combination of forest
765 inventory data with modelling of biomass, litter and soil. Ann For Sci 63:687-697.

766 Lung T, Dosio A, Becker W, Lavalle C, Bouwer LM (2013) Assessing the influence of climate model
767 uncertainty on EU-wide climate change impact indicators. Clim Change 120:211-227

768 Ma J, Yan X, Dong W and Chou J (2015) Gross primary production of global forest ecosystems has
769 been overestimated. Nature Sci Rep 5: 1-9

770 Mäkelä, A. and Valentine, H.T. (2001) The ratio of NPP to GPP: Evidence of change over the course
771 of stand development. Tree Phys 21:1015–1030.

772 Mäkelä A, Kolari P, Karimäki J, Nikinmaa E, Perämäki M, Hari P (2006) Modelling five years of
773 weather-driven variation of GPP in a boreal forest. Agric For Meteorol 139:382-398

774 Mäkelä A, Pulkkinen M, Kolari P, Lagergren F, Berbigier P, Lindroth A, Loustau D, Nikinmaa E,
775 Vesala T, Hari P (2008) Developing an empirical model of stand GPP with the LUE approach:
776 analysis of eddy covariance data at five contrasting conifer sites in Europe. Glob Change Biol 14:92-
777 108

778 Mäkelä A, Hari P, Berninger F, Hänninen H, Nikinmaa E (2004) Acclimation of photosynthetic
779 capacity in Scots pine to the annual cycle of temperature. Tree Physiol 24:369-376

780 Mäkelä A, Valentine HT, Helmisaari H-S (2008) Optimal co-allocation of carbon and nitrogen in a
781 forest stand at steady state. New Phyto 180: 114-123

782 Mäkelä A, Pulkkinen M, Mäkinen H (2016) Bridging empirical and carbon-balance based forest site
783 productivity - Significance of below-ground allocation. For Ecol Manage 372:64-77.

784 Medlyn BE, Duursma RA, Zeppel MJB (2011) Forest productivity under climate change: a checklist
785 for evaluating model studies. Wiley Interdisciplinary Reviews: Clim Change 2:332-355

786 Meehl GA, Covey C, Delworth T, Latif M, McAvaney B, Mitchell JFB, Stouffer RJ, Taylor KE
787 (2007) The WCRP CMIP3 multimodel dataset: A new era in climate change research. Bull Am
788 Meteorol Soc 88:1383-1394

789 Minunno F, Peltoniemi M, Launiainen S, Aurela M, Lindroth A, Lohila A, Mammarella I, Minkkinen
790 K, Mäkelä A (2016) Calibration and validation of a semi-empirical flux ecosystem model for
791 coniferous forests in the Boreal region. Ecol Model 341: 37 - 52

792 Moss RH, Edmonds JA, Hibbard KA, Manning MR, Rose SK, Vuuren DP van, Carter TR, Emori S,
793 Kainuma M, Kram T, Meehl GA, Mitchell JFB, Nakicenovic N, Riahi K, Smith SJ, Stouffer RJ,
794 Thomson AM, Weyant JP, Wilbanks TJ (2010) The next generation of scenarios for climate change
795 research and assessment. Nature 463:747–756

796 Muukkonen P, Nevalainen S, Lindgren M, Peltoniemi M (2015) Spatial occurrence of drought
797 associated damage in Finnish boreal forests: results from forest condition monitoring and GIS
798 analysis. Bor Env Res 20:172-180

799 Nishina K, Ito A, Falloon P, Friend AD, Beerling DJ, Ciais P, Clark DB, Kahana R, Kato E, Lucht W,
800 Lomas M, Pavlick R, Schaphoff S, Warsawaski L, Yokohata T (2015) Decomposing uncertainties in

the future terrestrial carbon budget associated with emission scenarios, climate projections, and ecosystem simulations using the ISI-MIP results. Earth Syst Dynam 6:435-445

Norby RJ, Zak DR (2011) Ecological Lessons from Free-Air CO2 Enrichment (FACE) Experiments. Ann Rev Ecol Evol Syst 42:181-203

Norby RJ, Warren JM, Iversen CM, Medlyn BE, McMurtrie RE (2010) CO2 enhancement of forest productivity constrained by limited nitrogen availability PNAS 107(45): 19368–19373

Novick KA, Oishi AC, Ward EJ, Siqueira MBS, Juang J-Y, Stoy PC (2015) On the difference in the net ecosystem exchange of CO2 between deciduous and evergreen forests in the southeastern United States. Glob Change Biol 21:827-842.

Ollikainen M (2014) Forestry in bioeconomy – smart green growth for the humankind. Scan J For Res 29:360-366

Ollinger SV, Goodale CL, Hayhoe K, Jenkins JP (2007) Potential effects of climate change and rising CO2 on ecosystem processes in northeastern U.S. forests. Mitig Adapt Strat Glob Change 13:476-485

Palacio S, Hoch G, Sala A, Körner C, Millard P (2014) Does carbon storage limit tree growth? New Phyto 201: 1096–1100

Peltola H, Ikonen VP, Gregow H, Strandman H, Kilpeläinen A, Venäläinen A, Kellomäki S (2010) Impacts of climate change on timber production and regional risks of wind-induced damage to forests in Finland. For Ecol Manage 260:833-845.

Peltoniemi M, Pulkkinen M, Kolari P, Duursma RA, Montagni L, Wharton S, Lagergren F, Takagi K, Verbeeck H, Christensen T, Vesala T, Falk M, Loustau D, Mäkelä A (2012) Does canopy mean nitrogen concentration explain variation in canopy light use efficiency across 14 contrasting forest sites. Tree Phys 32:200-218.

Peltoniemi M, Pulkkinen M, Aurela M, Pumpanen J, Kolari P, Mäkelä A (2015) A semi-empirical model of boreal forest gross primary production, evapotranspiration, and soil water – calibration and sensitivity analysis. Bor Env Res 20:151-171

Reich PB, Ellsworth DS, Walters MB (1998). Leaf structure (specific leaf area) modulates photosynthesis-nitrogen relations: evidence from within and across species and functional groups. Funct Ecol 12: 948-958

Reich PB, Rich RI, Lu X, Wang Y-P, Oleksyn J (2014) Biogeographic variation in evergreen conifer needle longevity and impacts on boreal forest carbon cycle projections. Proc Natl Acad Sci 111:13703-13708.

Reick CH, Raddatz T, Brovkin V, Gayler V (2013) Representation of natural and anthropogenic land cover change in MPI-ESM. J Adv Model Earth Syst 5:459-482

Reyer C, Lasch-Born P, Suckow F, Gutsch M, Murawski A, Pilz T (2014) Projections of regional changes in forest net primary productivity for different tree species in Europe driven by climate change and carbon dioxide Ann For Sci 71:211-225

Rötter RP, Höhn J, Trnka M, Fronzek S, Carter TR, Kahiluoto H (2013) Modelling shifts in agroclimate and crop cultivar response under climate change. Ecol Evol 3:4197-4214

839 Rummukainen M (2013) Climate change: changing means and changing extremes. Clim Change
840 121:3-13

841 Rummukainen M (2012) Changes in climate and weather extremes in the 21st century. WIREs Clim
842 Change 3:115-129

843 Ruosteenoja K, Räisänen J, Pirinen P (2011) Projected changes in thermal seasons and the growing
844 season in Finland. Int J Climatol 31:1437-1487

845 Ruosteenoja, K., Jylhä, K. and Kämäräinen, M. (2016) Climate Projections for Finland Under the
846 RCP Forcing Scenarios. Geophysica, 51:17-50

847 Seidl R, Thom D, Kautz M, Martin-Benito D, Peltoniemi M, Vacchiano G, Wild J, Ascoli D, Petr M,
848 Honkaniemi J, Lexer MJ, Trotsiuk V, Mairota P, Svoboda M, Fabrika M, Nagel TA, Reyer CPO
849 (2017) Forest disturbances under climate change. Nat Cli Change:395-402.

850 Sievänen R, Salminen O, Lehtonen A, Ojanen P, Liski J, Ruosteenoja K, Tuomi M (2014) Carbon
851 stock changes of forest land in Finland under different levels of wood use and climate change. Ann
852 For Sci 71: 255-265.

853 Snyder PK, Delire C, Foley JA (2004) Evaluating the influence of different vegetation biomes on the
854 global climate. Clim Dyn 23:279-302

855 Snyder PK, Liess S (2014) The simulated atmospheric response to expansion of the Arctic boreal
856 forest biome. Clim Dyn 42: 487–503

857 Storn R, Price K (1997) Differential Evolution — a simple and efficient heuristic for global
858 optimization over continuous spaces. J Global Optimi 11:341–359.

859 ter Braak CJF (2006) A Markov chain Monte Carlo version of the genetic algorithm differential
860 evolution: easy Bayesian computing for real parameter spaces. Stat Comput 16:239-249.

861 ter Braak CJ, Vrugt JA (2008) Differential evolution Markov chain with snooker updater and fewer
862 chains Stat Comput 18:435-446.

863 Uusitalo L, Lehikoinen A, Helle I, Myrberg K (2015) An overview of methods to evaluate uncertainty
864 of deterministic models in decision support. Environmental Modelling & Software 63: 24-31.

865 van Oijen M, Reyer C, Bohn FJ, Cameron DR, Deckmyn G, Felchsig M, Härkönen S, Hartig F, Huth
866 A, Kiviste A, Lasch P, Mäkelä A, Mette T, Minunno F, Rammer W (2013) Bayesian calibration,
867 comparison and averaging of six forest models, using data from Scots pine stands across Europe. For
868 Ecol Manage 289: 255–268.

869 van Vuuren … et al. (2011) The representative concentration pathways: an overview. Climatic
870 Change 109: 5-31

871 van Vuuren DP, Carter TR (2014) Climate and socio-economic scenarios for climate change research
872 and assessment: reconciling the new with the old. Clim Change 122:415–429.

873 Venäläinen A, Tuomenvirta H, Pirinen P, Drebs A (2005) A basic Finnish climate data set 1961–
874 2000-description and illustration. Finn Meteorol Inst Rep 5

Wagle P, Xiao X, Kolb TE, Law BE, Wharton S, Monson RK, Chen J, Blanken PD, Novick KA, Dore S, Noormets A, Gowda PH (2016) Differential responses of carbon and water vapor fluxes to climate among evergreen needleleaf forests in the USA. Ecol Process 5:8

Wamelink GWW, Wieggers HJJ, Reinds GJ, Kros J, Mol-Dijkstra JP, van Oijen M, de Vries W (2009) Modelling impacts of changes in carbon dioxide concentration, climate and nitrogen deposition on carbon sequestration by European forests and forest soils. For Ecol Manage 258:1794-1805

Waring RH, Landsberg JJ, Williams M (1998) Net primary production of forests: a constant fraction of gross primary production? Tree Phys 18:129–134.

Warren JM, Pötzelsberger E, Wullschleger SD, Thornton PE, Hasenauer H, Norby RJ (2011) Ecohydrologic impact of reduced stomatal conductance in forests exposed to elevated CO2. Ecohydrol 4:196-210

Veijalainen N, Lotsari E, Alho P, Vehviläinen B, Käyhkö J (2010) National scale assessment of climate change impacts on flooding in Finland. J Hydro 391:333-350.

Supplementary material A: Climate scenarios and derivation of weather variables

Table SA1. List of General Circulation Model (GCM) simulations from the CMIP5 project for the RCP2.6, RCP4.5 and RCP8.5 scenarios, and from the CMIP3 archive (Meehl *et al.*, 2007) for three SRES emission scenarios (B1, A1B, A2) (Nakicenovic *et al*. 2000, IPCC 2007, Table 8.1).

Pathway/Scenario	GCM	Institution
RCP	CanESM2	Canadian Centre for Climate Modelling and Analysis
	CNRM-CM5	Centre National de Recherches Meteorologiques / Centre Europeen de Recherche et Formation Avancees en Calcul Scientifique
	GFDL-CM3	Geophysical Fluid Dynamics Laboratory
	HadGEM2-ES	Met Office Hadley Centre (additional HadGEM2-ES realizations contributed by Instituto Nacional de Pesquisas Espaciais)
	MIROC5	Atmosphere and Ocean Research Institute (The University of Tokyo), National Institute for

		Environmental Studies, and Japan Agency for Marine-Earth Science and Technology
SRES	BCCR-BCM2.0	Bjerknes Centre for Climate Research, Norway
	CCCMA-CGMC3.1(T47)	Canadian Centre for Climate Modelling and Analysis
	CNRM-CM3	Météo-France
	CSIRO-Mk3.5	CSIRO Atmospheric Research, Australia
	GISS-ER	Goddard Institute for Space Studies, USA
	INM-CM3.0	Institute for Numerical Mathematics, Russia
	IPSL-CM4	Institut Pierre Simon Laplace, France
	MIROC3.2 (medres)	Center for Climate System Research, National Institute for Enviromental Studies and Frontier Research Center for Global Change, Japan

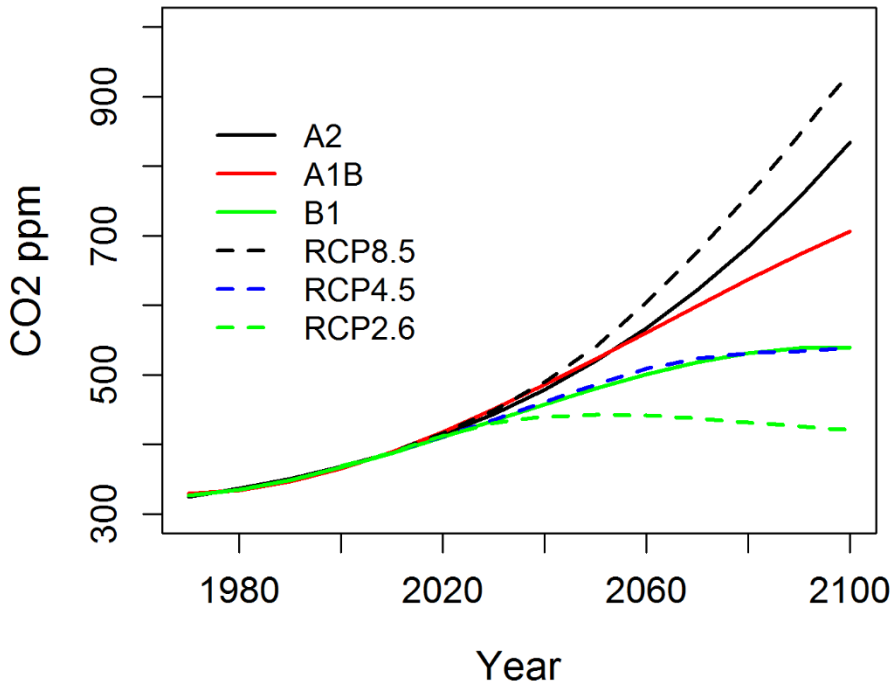

Figure SA.1 The development of atmospheric CO2 concentrations (C_a in ppm) in atmosphere over the 21st century. RCP2.6 by integrated assessment model IMAGE, RCP4.5 by MiniCAM, and RCP8.5 by

MESSAGE. SRES curves (A2, A1B, B1) were drawn with parameters fitted on estimates of BERN carbon cycle model (IPCC, 2007).

On the differences between bias correction and delta change approaches

The main difference between these two methods is that the bias correction method is based on the modelled climate whereas delta change method uses historical data. This difference means that in delta change method the observed interannual variability does not change in the projected future climate while in bias correction temporal properties such as autocorrelation could change over time and thus interannual variability may change in the projected climate from the historical one. From the viewpoint of ecological impact study, the delta change method could be more relevant in near-term projections, e.g. up to 2040, and especially if expected changes in the phenomena of interest are small. The bias correction method is regarded more preferable for the projections of further in the future, e.g. 2050-2100., or where expected changes are large.

Estimation of water vapour pressure deficit, VPD

For the model simulations, we converted grid estimates of daily vapour pressures to vapour pressure deficits (VPD) according to Cambell and Norman (2000).

Water vapour pressure deficit (Pa) is given by the difference between actual water vapour pressure e_a and its saturation value e_s

$$VPD = e_a - e_s$$

The vapour pressure of saturated air was obtained from the Tetens formula

$$e_s(T) = a \times \exp(\frac{bT}{T + c})$$

where T is temperature, and constants are a = 0.611, b = 17.502, and c = 240.97.

In the scenario climate i, new actual water vapour pressure e_{ai} was calculated from the observed vapour pressures (VP_a) and vapour pressure deltas (ΔVP_i) obtained from same ensemble of 8 GCMs as temperature deltas (ΔT_i).

$$e_{ai} = VP_a + \Delta VP_i$$

Saturated vapour pressure e_{si} in the scenario climate i was calculated accordingly

$$e_{si} = e_s(T + \Delta T_i)$$

Thereafter, VPD in scenario climate i was obtained from

$$VPD_i = e_{si} - e_{ai}$$

The obtained VPDs are presented in Figure SA2. The scenarios of climate change by climate model used in the gross primary productions (P) simulations are given for southern and northern (south and north from 65°N) Finland separately. The entire latitudinal range of Finland is 59°30'N - 70°05'N.

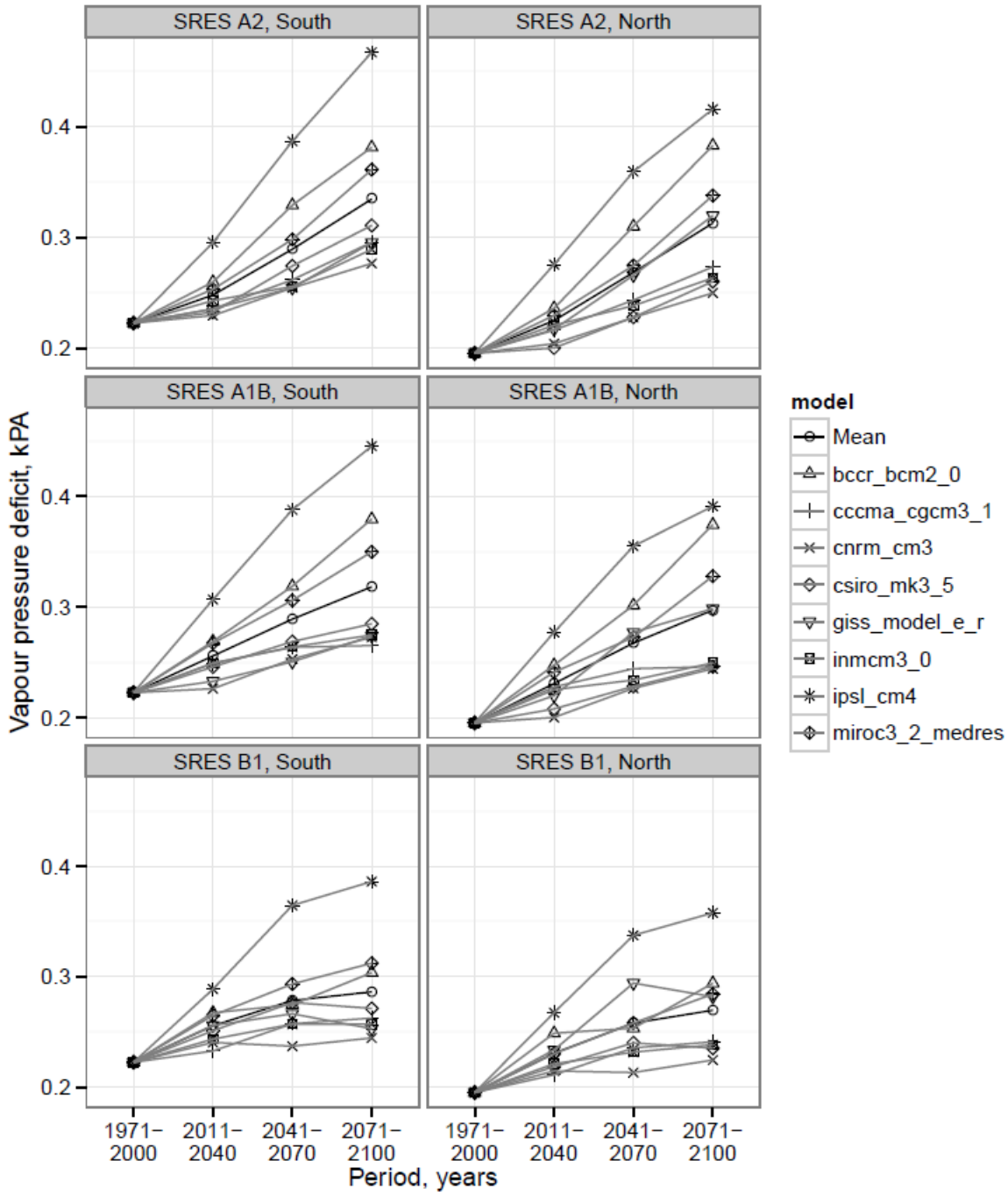

Figure SA.2 Scenarios of annual VPD in southern and northern Finland using eight climate models, and their average estimate during the 30 year periods.

Photosynthetic photon flux density, PPFD

Reference period values of global radiation did not represent plausible interannual variation. Therefore we produced reference period radiation data in SRES projections with the method presented in Oker-Blom et al. 1989 based on the sun elevation. We applied this method for each day and hour of the year and calculated theoretical clear sky radiation, which we further converted to estimates of actual PPFD, based on its relationship with weather variables in Hyytiälä. The following decomposition of actual PPFD was used:

$$\phi = \phi_m + \phi_D + \varepsilon_i$$

where ϕ_m is the mean overall daily ϕ estimated from hourly (k) sun radiations ξ_k estimated with the method of Oker-Blom et al. (1989)

$$\phi_m = c_m \sum_{k=0}^{23} \xi_k$$

Integrating diurnal hourly values of theoretical radiation yielded daily theoretical PPFD (ϕ_t), which was converted to mean daily PPFD by multiplication with a fitted coefficient, c_m=2.051,

$$\phi_m = c_m \phi_t.$$

To represent co-variation of PPFD with daily weather, we added a second term to the model that represented VPD-dependency of ϕ:

$$\phi_D = \frac{a_1}{a_2 D + 1} - a_3$$

where all a are fitted coefficients. Residuals of this fit has a seasonal D relationship, so we finally replaced the ε_i term with their means estimated for four types of days, those with high and low sun mean radiation (ϕ_m < 5 mol m-2), ϕ_m < 5 mol m-2, respectively) and high and low VPD (D < 0.1 kPa and D < 0.1 kPa).

The obtained radiation is presented in Figure SA3. The scenarios of climate change by climate model used in the gross primary productions (P) simulations are given for southern and northern (south and north from 65°N) Finland separately. The entire latitudinal range of Finland is 59°30'N - 70°05'N.

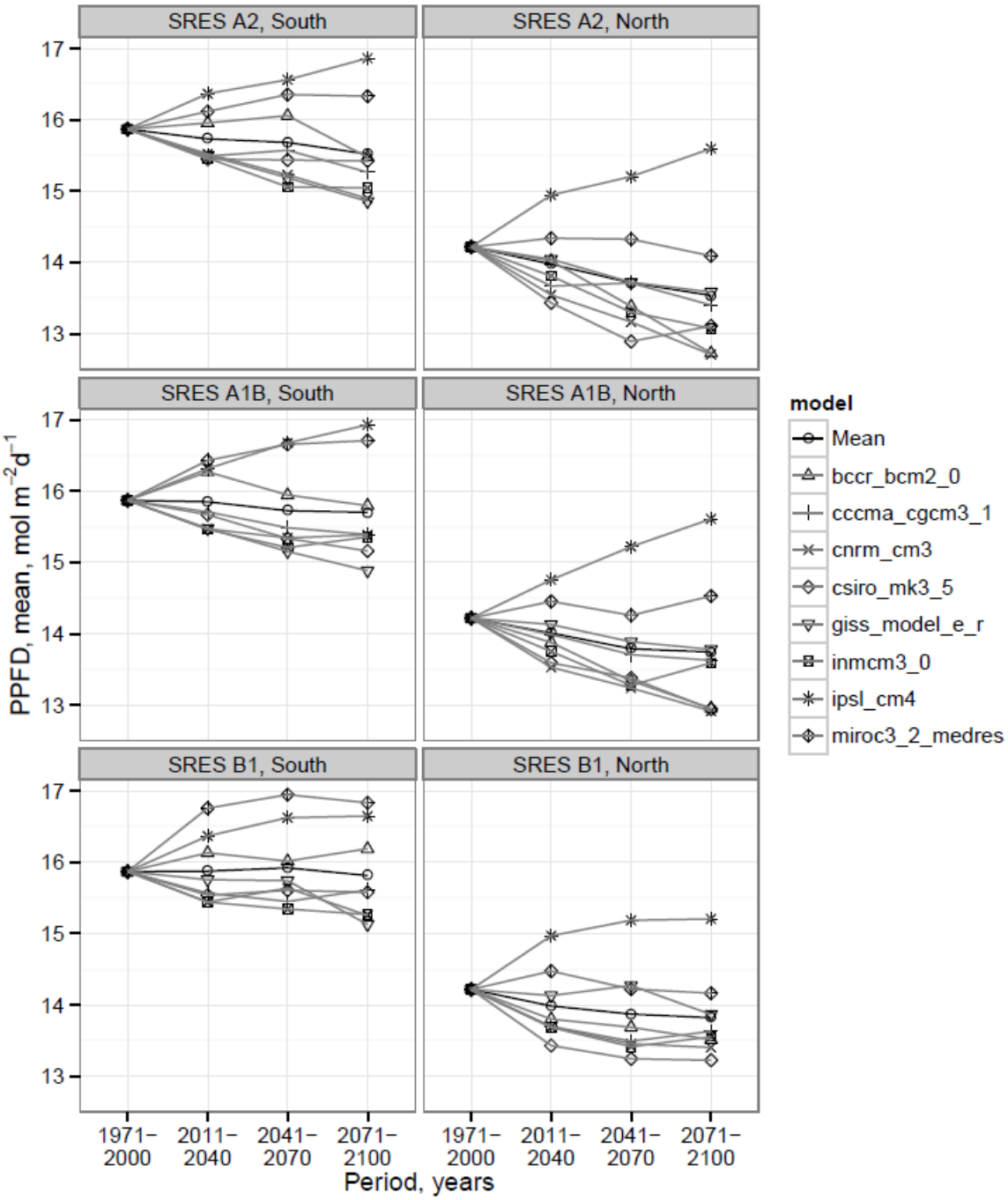

990

991 Figure SA.3 Scenarios of annual radiation in southern and northern Finland using eight climate models,
992 and their average estimate during the 30 year periods.

993

994

995

Effective temperature sum, ETS

We calculated effective temperature sum as the sum of degrees by which the daily average temperature exceeds +5 °C. A threshold of +5 °C is a commonly used standard when calculating the effective temperaturesum in forestry and agriculture in the Nordic countries. Figure SA4 shows the development of annual temperature sum projected by different climate models.

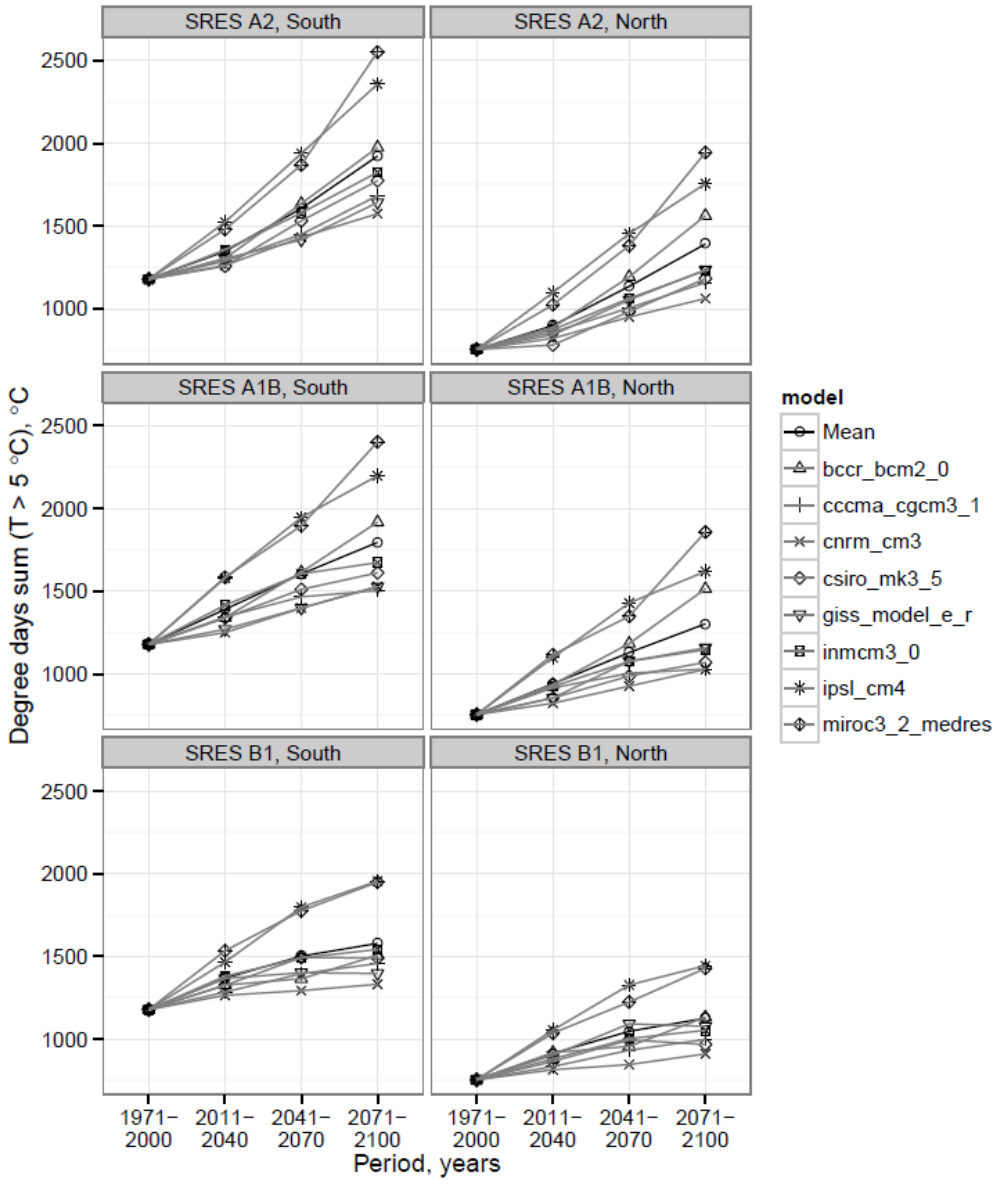

Figure SA.4 Scenarios of annual temperature sum in southern and northern Finland using eight climate models, and their average estimate during the 30 year periods.

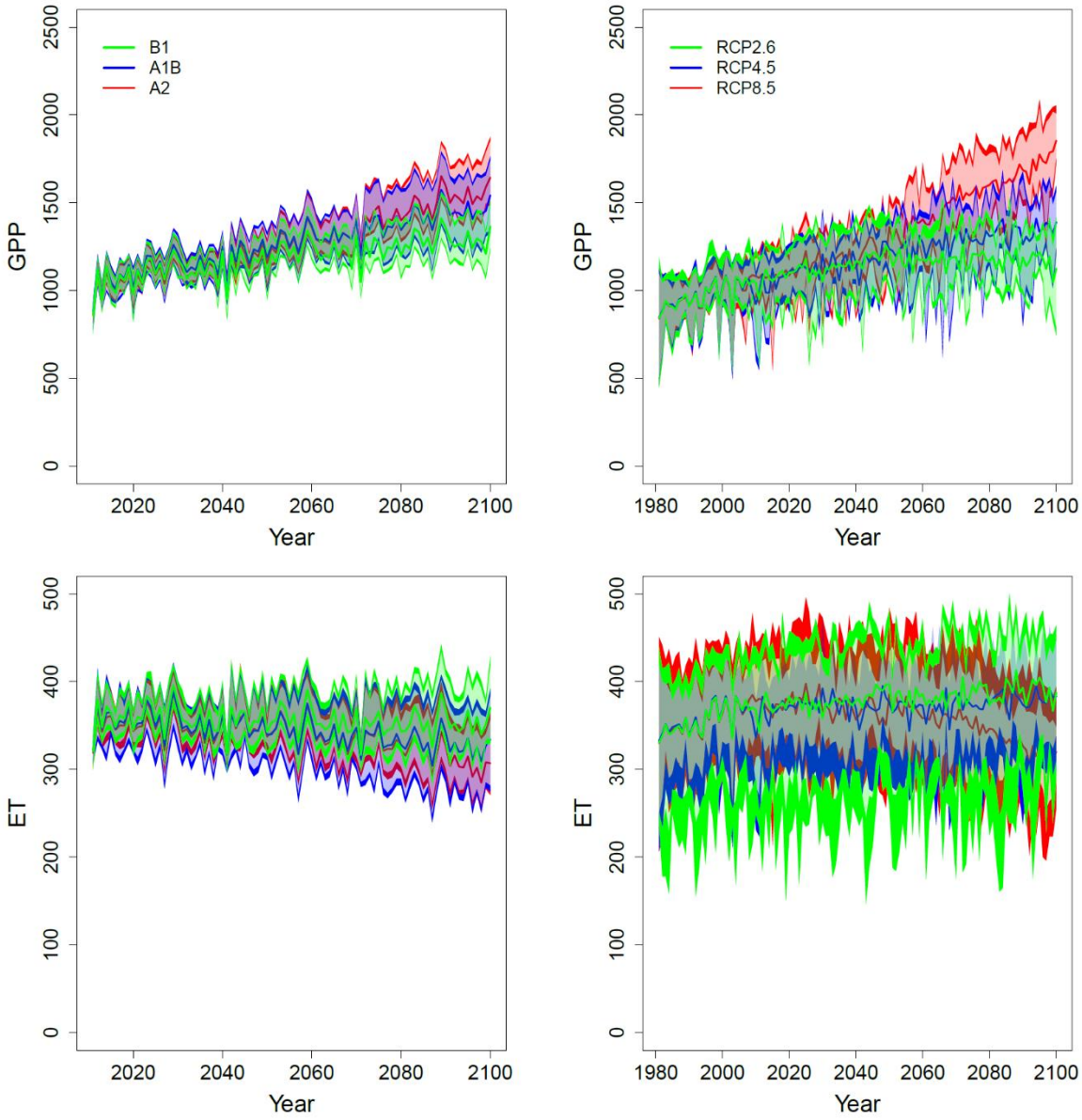

Figure SA.5 The emission scenario/pathway specific gross primary production (GPP) and evapotranspiration (ET). The lighter shade of the coloured area around each curve shows the GCM variability and the outermost darker shade indicates PRELES parametric and structural uncertainty within each emission scenario.

References

Campbell GS, Norman JM (2000) Introduction to environmental biophysics. 2nd Ed. Springer-Verlag New York, lnc.

IPCC (2007) Climate Change 2007: The Physical Science Basis. Contribution of Working Group I to the Fourth Assessment Report of the Intergovernmental Panel on Climate Change. Cambridge University Press, Cambridge, United Kingdom and New York, NY, USA

Meehl GA, Covey C, Taylor KE, Delworth T, Stouffer RJ, Latif M, McAvaney B, Mitchell JFB (2007) The WCRP CMIP3 Multimodel Dataset: A New Era in Climate Change Research. Bull of the Am Met Soc 88:1383–1394. doi:10.1175/BAMS-88-9-1383.

Nakicenovic N, Alcamo J, Davis G, 25 others (2000) Special report on emissions scenarios: a special report of Working Group III of the Intergovernmental Panel on Climate Change. Cambridge University Press, Cambridge; New York.

Oker-Blom P, Pukkala T, Kuuluvainen T (1989) Relationship between radiation interception and photosynthesis in forest canopies: effect of stand structure and latitude. Ecol Mod 49: 73 – 87.

Supplementary material B: Model responses to synthetic climate forcing

The model predicts increases of P with increasing C_a, which slightly saturate under high C_a (Fig. SB.1). The absolute increases are proportional to f_{aPPFD}. Changes are more pronounced under high D. The

model predicts decreases of E with increasing C_a (Fig. SB.2). The absolute increases are proportional to f_{aPPFD}. Changes are more pronounced under high f_{aPPFD}, where the fraction of transpiration of E is larger. The changes of P and E lead to increase of ecosystem WUE (water use efficiency, P/E), which are nearly linear (Fig. SB.3). We also applied the model with Hyytiälä eddy-covariance site weather data, in order to show how model predicts under hypothetical weather scenarios whereby we modified the input variables in a systematic manner (Fig. SB.4). Assuming that precipitation does not increase, T and PAR remain unchanged, we find an increase of annual mean P from 2.7 to 3.4 gC m^{-2} d^{-1} when C_a increases from 380 to 700 ppm. If this change is accompanied with an increase of 5° C in all annual daily temperatures, the corresponding increase of P is from 3.05 to 4.2 gC m^{-2} d^{-1}. Under increasing T, the role of precipitation increases, due to the increasing evapotranspiration and decreasing soil moisture content (not shown). If irradiance upon canopies decreases, the role of soil moisture limitation decreases. Effects of C_a have been implemented in the form of empirical equations fitted to a detailed stand level model that implements the biochemical photosynthesis model (Farquhar et al. 1980, Leuning 1995). Our model predicted 11 and 15% increase of P and E when exposed to 550 ppm (D = 0.5 kPa, f_{aPPFD} = 1) (*ceteris paribus*). Light-use efficiency should increase 25% when C_a increases from current levels to 550 ppm in a closed canopy forest without the effects of photosynthetic down-regulation (Medlyn et al. 2011). Warren et al. (2011) found in a FACE experiment that the annual canopy transpiration decreased 10-16% due to elevated C_a, while in a multimodel comparison the range of stand transpiration among models was from -31 to +10% (De Kauwe et al. 2013). Our model estimates are, thus, roughly comparable to these.

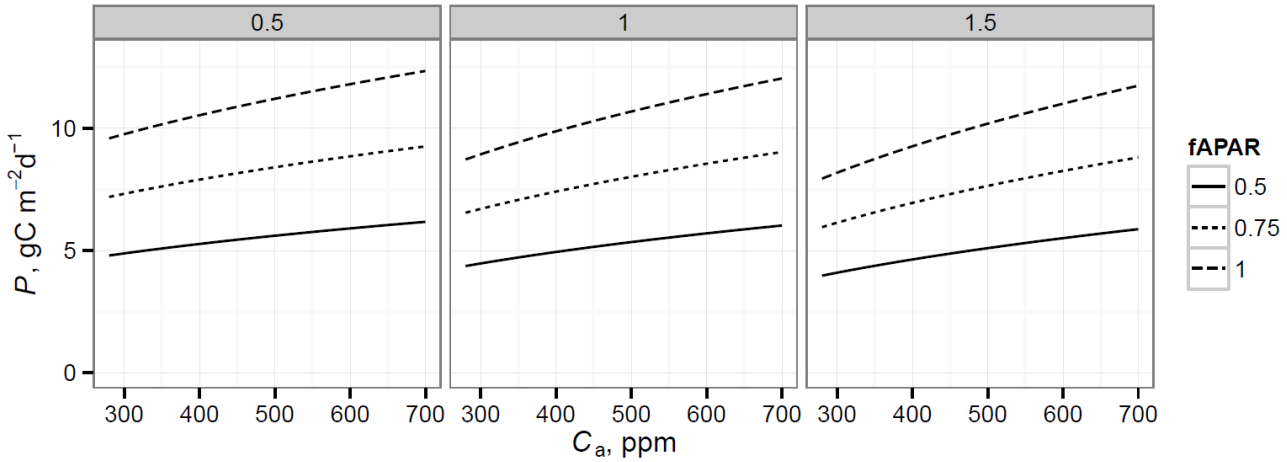

1064

1065 Figure SB.1 Increase of model predicted daily *P* with increasing C_a and by *D* and f_{APAR}. The values of
1066 *D* on the upper grey panel (0,5 – 1,5). In these simulations, the effect of *T* and seasonality term of the
1067 model (*S*) was saturated, and soil moisture did not play role. PAR upon canopy was set to 30 mol/m2.
1068 Default model parameters (for Scots pine) were used.

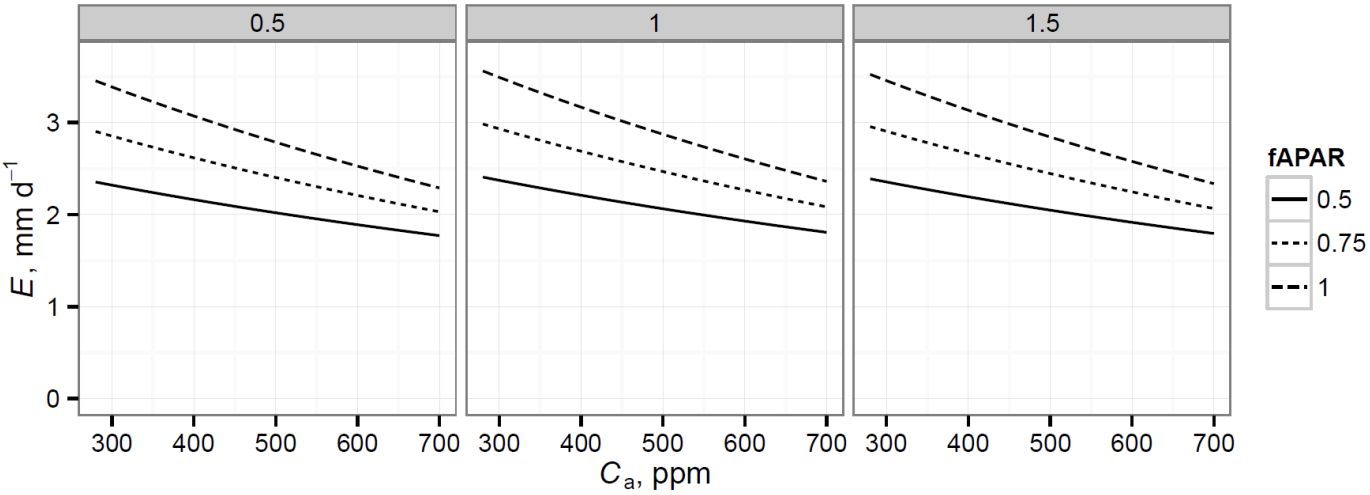

1069

1070 Figure SB.2 Change of model predicted daily *E* with increasing C_a and by *D* and f_{APAR}. The values of
1071 *D* on the upper grey panel (0,5 – 1,5). In these simulations, the effect of *T* and seasonality term of the
1072 model (*S*) was saturated, and soil moisture did not play role. PAR upon canopy was set to 30 mol/m2.
1073 Default model parameters (for Scots pine) were used.

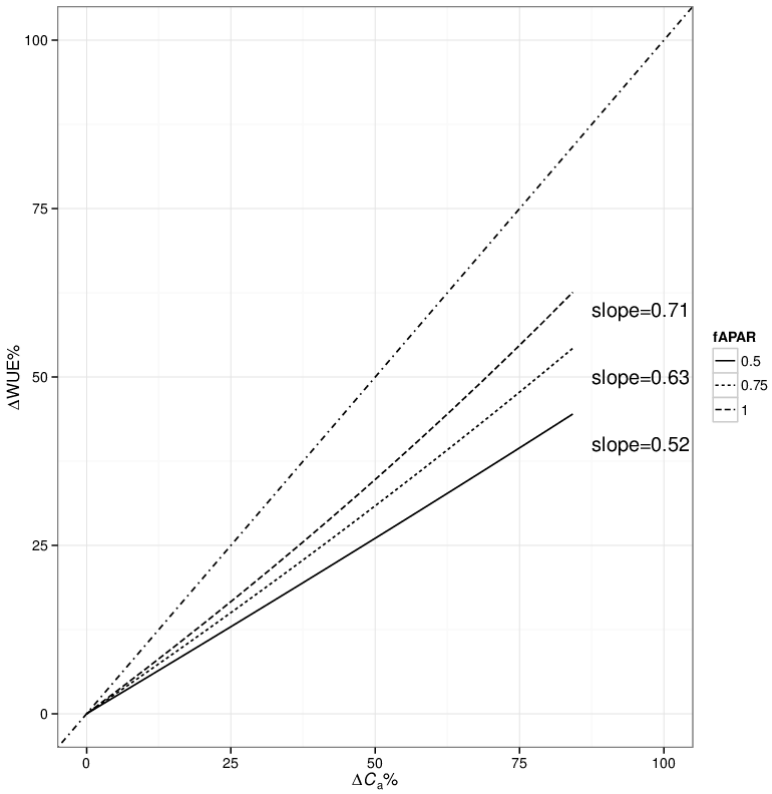

Figure SB.3 Relative change of ecosystem WUE with relative change of C_a at different f_{APAR}. Dash dot line is the 1:1 relationship. *D* was set to constant 0.5 kPA, air temperature to 20 C and PAR to 30 mol/m2. WUE is sensitive to *D*: slope at f_{APAR} = 1 increases from 0.63 to 0.97 when daily average *D* increases from 0 to 2 kPA.

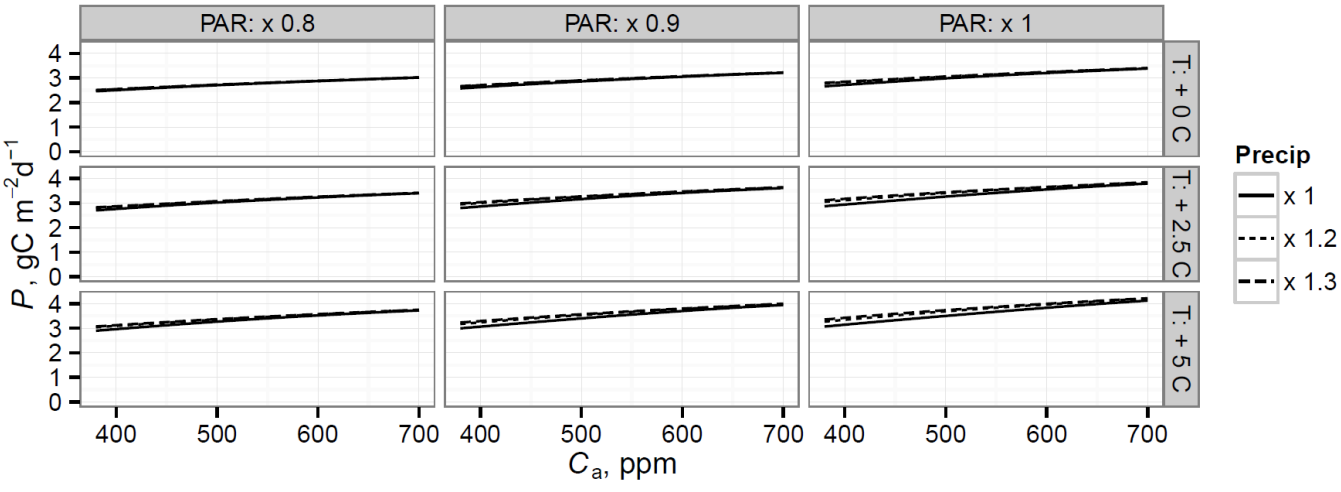

Figure SB.4 Annual mean *P* (across simulation period of 10 years) in Hyytiälä. Default model parameters (for Scots pine) were used.

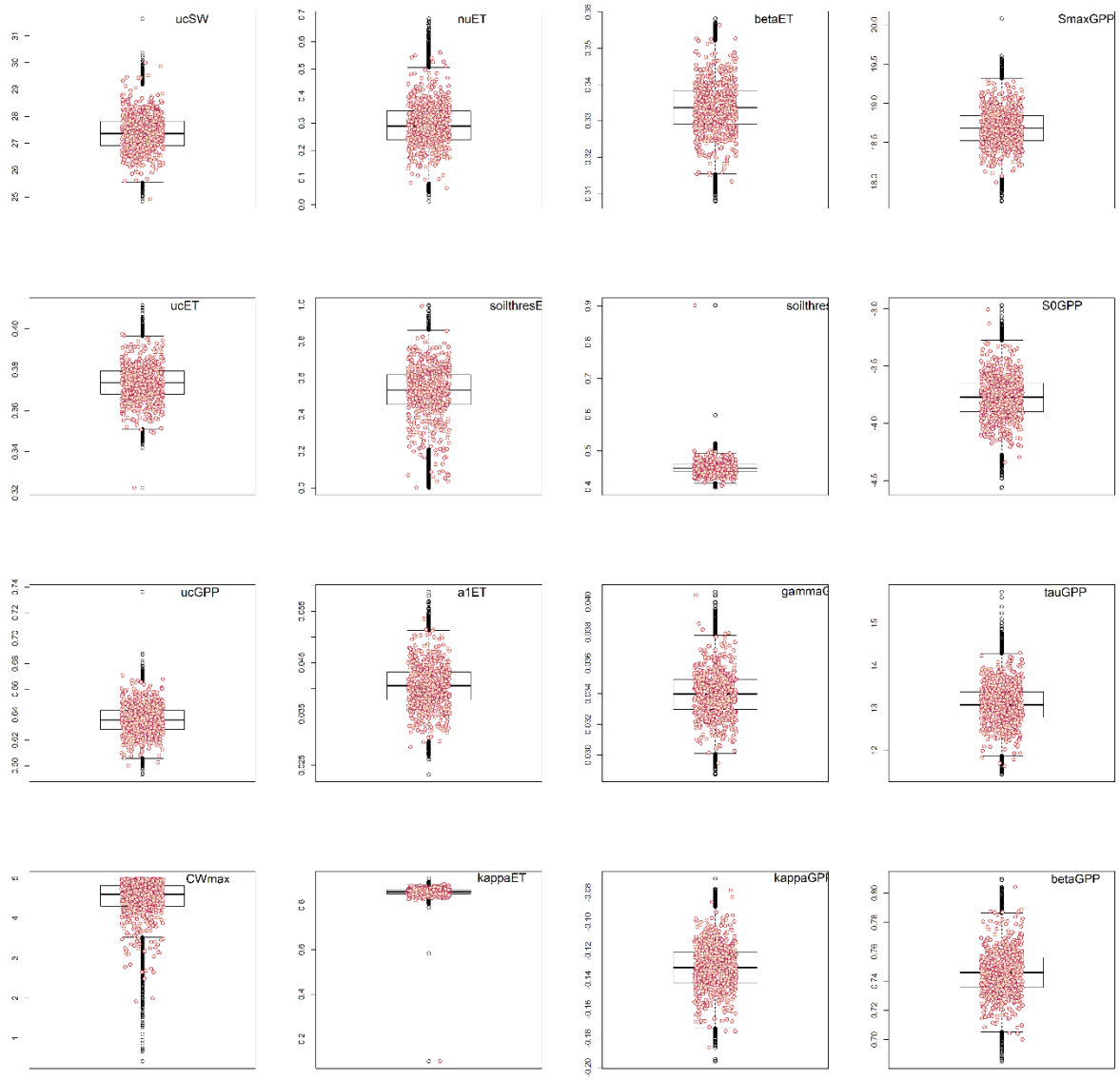

Figure SB.5 The boxplot of each parameter showing the total variation of posteriori. Red circles indicate the parameter values sampled from the posteriori for the description of PRELES parametric uncertainty in the simulations.

References

De Kauwe MG, Medlyn BE, Zaehle S, Walker AP, Dietze MC, Hickler T, Jain AK, Luo Y, Parton WJ, Prentice IC, Smith B, Thornton PE, Wang S, Wang Y, Wårlind D, Weng E, Crous KY, Ellsworth DS, Hanson PJ, Seok Kim H, Warren JM, Oren R, Norby RJ (2013) Forest water use and water use efficiency at elevated CO2: a model-data intercomparison at two contrasting temperate forest FACE sites. Glob Change Biol 19:1759-1779

Farquhar GD, Caemmerer S, Berry J (1980) A biochemical model of photosynthetic CO_2 assimilation in leaves of C3 species. Planta 149:78-90

1095 Medlyn BE, Duursma RA, Zeppel MJB (2011) Forest productivity under climate change: a checklist
1096 for evaluating model studies. Wiley Interdisciplinary Reviews: Clim Change 2:332-355

1097 Leuning R (1995) A critical appraisal of a combined stomatal-photosynthesis model for C3 plants.
1098 Plant Cell Env 18:339-355

1099 Warren JM, Pötzelsberger E, Wullschleger SD, Thornton PE, Hasenauer H, Norby RJ (2011)
1100 Ecohydrologic impact of reduced stomatal conductance in forests exposed to elevated CO2.
1101 Ecohydrol 4:196-210

1102

1103